Acta Geologica Polonica, Vol. 56 (2006), No. 4, pp. 375-405

Buckle folding in the Kielce Unit, Holy Cross Mountains, central Poland

ANDRZEJ KONON

Institute of Geology, University of Warsaw, Żwirki i Wigury Str., 93, PL-02-089 Warszawa, Poland.
E-mail: Andrzej.Konon@uw.edu.pl

ABSTRACT:

KONON, A. 2006. Buckle folding in the Kielce Unit, Holy Cross Mountains, central Poland. *Acta Geologica Polonica*, **56** (4), 375-405, Warszawa.

Gradual changes of shape profiles of map-scale as well as mesoscopic folds, recognised as symmetric and asymmetric buckle folds, were investigated. These folds developed in the Holy Cross Mountains in Palaeozoic unmetamorphosed sedimentary rocks during Variscan deformation. During folding, layer-parallel shortening prevailed, although a layer-parallel shear component, resulting from deformation of multilayers by compression at low angles to the layering, has also been recognized. Different contraction and extension fault sets, as well as cleavage, small-scale duplexes, boudinage and stylolites, developed progressively on both gradually steepening limbs of the symmetric folds, as well as mainly on the short limbs of the asymmetric folds. Based on the comparison of laboratory data for different types of rocks, the range of values of horizontal compressive stress levels occurring during fold growth has been estimated. The stress levels for the high pore fluid pressures probably did not exceed 150 MPa. These conditions and temperatures below 150°C favoured buckle folding. In the late phase of the folding or in the post-folding stage of Variscan deformation, the separation of the Kielce Unit into fault-bounded block domains was initiated along longitudinal and transverse faults. This resulted in changes in trend of parts of the map-scale folds.

Key words: Buckle folds, Faults sets, Compressive stress levels, Pore fluid pressures, Fault-bounded block domains, Variscan deformation, Holy Cross Mountains.

INTRODUCTION

The aim of the paper is to describe the folds from part of the Holy Cross Mountains (HCM) fold belt occurring in the Kielce Unit, including their geometry, stages of development and estimates of the condition of their origin. Additionally, among mesostructures, mainly the faults associated with the progressive shape modifications of such folds were analysed.

Folds typical of fold belts can be divided into at least four main types: fault-bend folds, fault-propagation folds, detachment folds and break-thrust folds (e.g. JAMISON 1987; THORBJORNSEN & DUNNE 1997). The folds in the HCM formed in unmetamorphosed sedimentary rock sequences comprising alternating competent and incompetent layers. When such folds form as a result of buckling, numerous mesostructures can develop on their limbs. In the hinges of these asymmetric

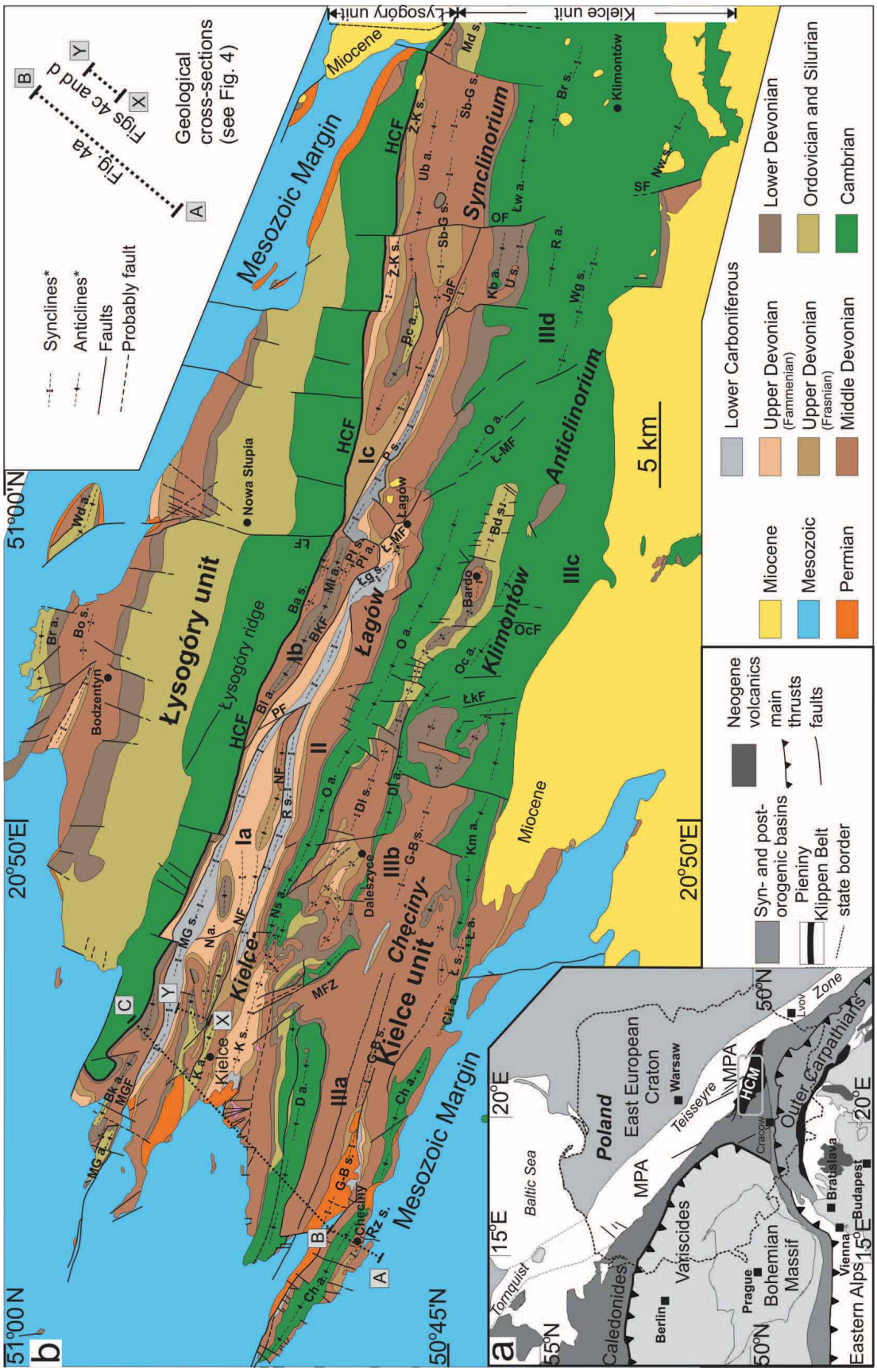
b
a
Geological cross-sections (see Fig. 4)
Fig. 4a
Figs 4c and d
Synclines*
Anticlines*
Faults
Probably fault
Łysogóry unit
Kielce unit
Mesozoic Margin
Miocene
Synclinorium
Anticlinorium
Łysogóry ridge
Kielce unit
Chęciny-Kielce unit
Łagów
Klimontów
HCF
IIIa
IIIb
IIIc
IIId
Ia
Ib
Ic
II
5 km
51°00'N
50°45'N
20°50'E
Nowa Słupia
Bodzentyn
Daleszyce
Chęciny
Kielce
Bardo
Klimontów
Lower Carboniferous
Upper Devonian (Fammenian)
Upper Devonian (Frasnian)
Middle Devonian
Lower Devonian
Ordovician and Silurian
Cambrian
Miocene
Mesozoic
Permian
Neogene volcanics
main thrusts
faults
Syn- and post-orogenic basins
Pieniny Klippen Belt
state border
Baltic Sea
Poland
East European Craton
Warsaw
Teisseyre
MPA
HCM
Cracow
Lviv
Outer Carpathians
Caledonides
Variscides
Bohemian Massif
Prague
Berlin
Vienna
Bratislava
Budapest
Eastern Alps
Tornquist
Zone
55°N
50°N
15°E
20°E

and symmetric folds, commonly with chevron profiles, can develop different accommodation structures e.g. limb thrusts or hinge collapses (RAMSAY 1967, 1974; RAMSAY & HUBER 1987; PRICE & COSGROVE 1990). The limb thrusts can form conjugate fault systems similar to faults in diapiric folds (DE SITTER 1964, fig. 120), also termed conjugate movement horizons (HORNE & CULSHAW 2001). A flexural-slip mechanism is commonly observed during the initial phases of folding of the complex multilayers before folds lock preceding flattening (e.g. DE SITTER 1964; RAMSAY 1967, 1974). Structures can develop on the fold limbs, including flexural-slip duplexes (TANNER 1989, 1992), domino structures (HORNE & CULSHAW 2001), shear fibre steps on layer surfaces (TANNER 1989) and drag folds.

In later stages of folding, the folds shapes can change from symmetrical to asymmetrical, involving limb and/or hinge rotation. Fault sets may develop on the limbs of symmetric as well as asymmetric folds from the phase of pre-buckling shortening until the next phases of fold amplification. Faulting resulting from gradual shape modifications of natural examples of such folds and conditions favouring such deformation have been investigated during this study in Devonian rocks of the southern part of the HCM (Text-figs 1-2).

Geological setting

The Holy Cross Mountains (HCM) are located within the Trans-European Suture Zone, that separates the East European Craton from younger foldbelts of Central Europe (BERTHELSEN 1993) (Text-fig. 1a). The HCM comprise a Palaeozoic massif, made up of the Łysogóry (northern) and Kielce (southern) tectono-stratigraphic units (CZARNOCKI 1919, 1957; POŻARYSKI 1978) (Text-figs 1b and 2b). According to POŻARYSKI (1969, fig. 1), POŻARYSKI & TOMCZYK (1993), and UNRUG & *al.* (1999), the Kielce Unit is the northern part of the Małopolska block which is bordered by the Holy Cross Fault on the north (Text-figs 1b and 2, HCF – Holy Cross Fault) (e.g. TOMCZYK 1988; POŻARYSKI 1990; POŻARYSKI & *al.* 1992; LAMARCHE & *al.* 2000, 2003; MASTELLA & MIZERSKI 2002). The Łysogóry Unit was described as part of the East European Craton (TOMCZYK 1988) or as an individual terrane (POŻARYSKI & TOMCZYK 1993; UNRUG & *al*. 1999). Recent deep seismic sounding experiments (CELEBRATION 2000) show that the Łysogóry Unit and Kielce Unit, along with the rest of the Małopolska Block, have an identical crustal structure and are connected with the East European Craton (the palaeocontinent of Baltica) (MALINOWSKI & *al.* 2005).

The rocks in the Kielce and Łysogóry units had undergone folding (CZARNOCKI 1919, 1957) as a result of N-S to NNE-SSW shortening during Variscan deformation after the Viséan, probably during the Late Carboniferous (e.g. CZARNOCKI 1950, 1957; TOMCZYK 1988; MIZERSKI 1995; LAMARCHE & *al*. 1999, 2002). Subsequently, the area of the HCM was a part of the Rift Basin (KUTEK 2001). Presently, the HCM constitutes a part of the Mid-Polish Anticlinorium (Text-fig. 1a, MPA), which developed as a result of the Maastrichtian-Paleocene inversion of the Rift Basin (KUTEK & GŁAZEK 1972; KUTEK 2001).

The investigations were carried out in numerous quarries in the Kielce Unit (Text-fig. 2a, active and closed-down quarries 1-28) and natural outcrops in Devonian carbonates and clastic rocks.

Fig. 1 a – Tectonic sketch-map of Central Europe (simplified after GUTERCH & *al.* 2000). MPA – Mid-Polish Anticlinorium, HCM – Holy Cross Mountains. b – Geological map of the Holy Cross Mountains (after CZARNOCKI 1938, 1961a-f; FILONOWICZ 1973a, modified). Folds in the Kielce Unit (from the north) – Ia block: Bk a. – Bukowa Anticline, MG s. – Miedziana Góra Syncline, N a. – Niewachlów Anticline; Ib block: Ba s. – Bartoszowiny Syncline, Bl a.– Bieliny Anticline, Mł a. – Małacentów Anticline, Pł s. – Płucki Syncline, Pł a. – Płucki Anticline; Ic block: Ż-K s. – Żerniki-Karwów Syncline, Bc s. – Baćkowice Anticline, Sb-G s. – Sobiekurów-Grocholice Syncline, Ub a. – Ublinek Anticline, Md s. – Międzygórz Syncline; IIa and IIb blocks: K a. – Kielce Anticline, K s. – Kielce Syncline, R s. – Radlin Syncline; IIc block: Łg s. – Łagów Syncline; IId block: P s. – Piotrów Syncline, Kb a. – Kabza Anticline, U s. – Ujazd Syncline; IIIa block: D a. – Dyminy Anticline, G-B s. – Gałęzice-Bolechowice Syncline, Ch a. – Chęciny Anticline, Rz s. – Rzepka Syncline, Zb a. – Zbrza Anticline; IIIb block: Ns a. – Niestachów, O a. – Orłowiny Anticline, Dl s. – Daleszyce Syncline, Dl a. – Daleszyce Anticline, G-B s. – Gałęzice-Bolechowice Syncline, Km a. – Komórki Anticline, Ł s. – Łabędziów Syncline, Ł a. – Łabędziów Anticline; IIIc block: O a. – Orłowiny Anticline, Bd s. – Bardo Syncline, Oc a. Ociesęki Anticline; IIId block: O a. – Orłowiny Anticline, R a. – Radwan Anticline, Wg s. – Wygiełzów Syncline, Łw a. – Łownica Anticline, Br s. – Beradz Syncline, Nw s. – Nawodzice Syncline. Folds in the Łysogóry Unit: Br – Bronkowice Anticline, Bo – Bodzentyn Syncline, Wd – Wydryszów Anticline. Main faults in the Holy Cross Mountains (from the north): HCF – Holy Cross Fault, ŁF – Łysogóry Fault, MGF – Miedziana Góra Fault, NF – Niewachlów Fault, PF – Porąbki Fault, BKF – Bieliny Kapitulne Fault, JaF – Jańczyce Fault, MFZ – Mójcza Fault Zone, ŁkF – Łukawki Fault, Ł-MF – Łagów-Michałów Fault, OF – Oziębłów Fault, SF – Samotnia Fault. For other explanations see text

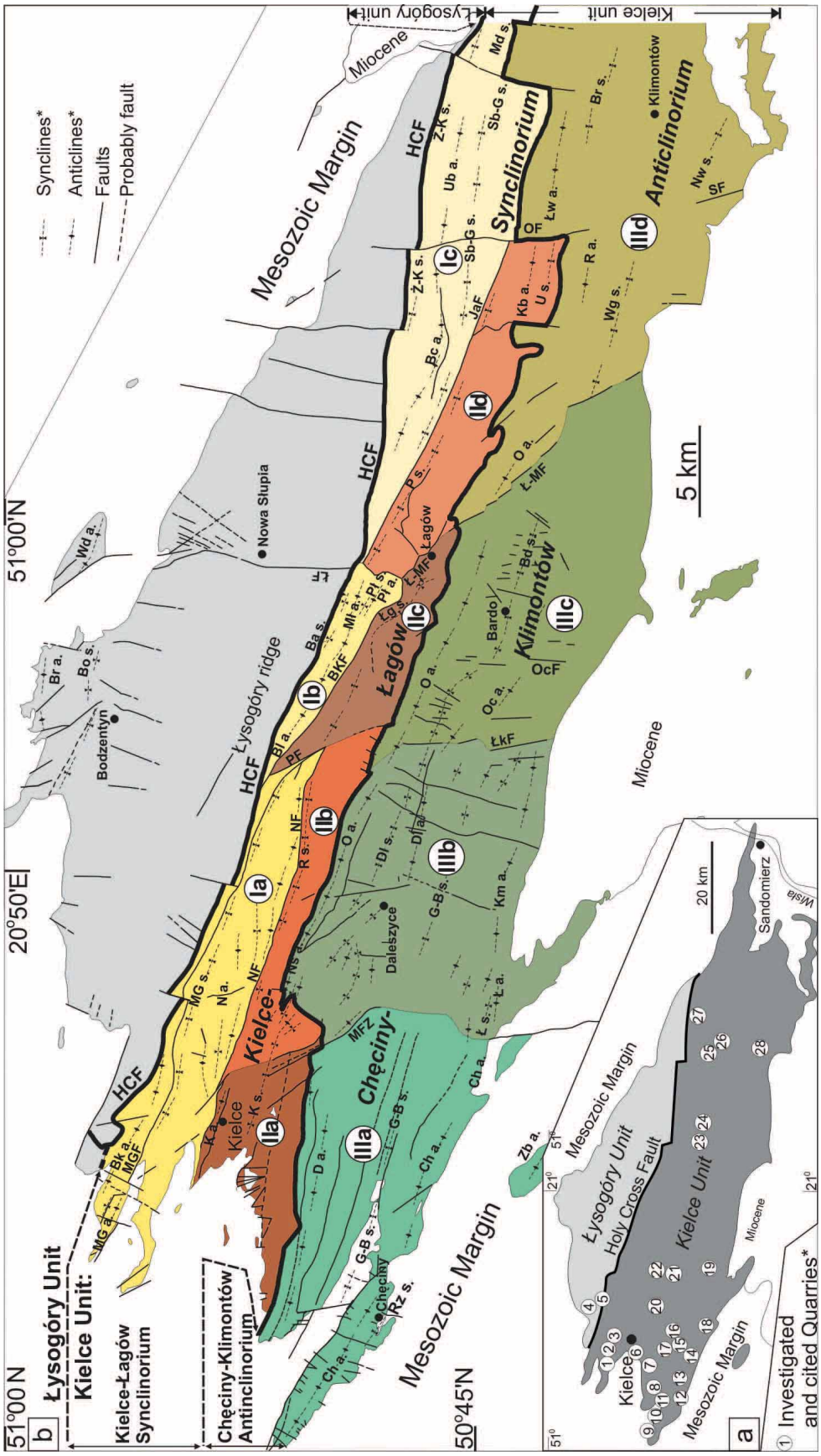
Synclines*
Anticlines*
Faults
Probably fault
Lysogóry unit
Kielce unit
Miocene
Mesozoic Margin
HCF
Synclinorium
Anticlinorium
Klimontów
Nowa Słupia
Bodzentyn
Lysogóry ridge
Łagów
Kielce
Chęciny-
Daleszyce
Sandomierz
Wisła
51°00'N
20°50'E
50°45'N
5 km
20 km
Lysogóry Unit
Kielce Unit:
Kielce-Łagów Synclinorium
Chęciny-Klimontów Antiinclinorium
Holy Cross Fault
Investigated and cited Quarries*

Lithostratigraphical units and their current mechanical properties

The mechanical rock properties control the shape of fold profiles and determine to a large extent the style of folding. These properties during the time of Variscan folding could be estimated only approximately with their current properties. Investigations of PINIŃSKA (1994, 1995) have shown that rocks selected in the Kielce Unit strongly differ from each other in their current mechanical properties.

The Kielce Unit includes Cambrian to Carboniferous unmetamorphosed silico-clastic as well as carbonate competent and incompetent rocks (Text-fig. 3). They include weak rocks represented by Cambrian, Silurian and Carboniferous shale and thin-bedded sandstone, strong Ordovician and Devonian dolomite and limestone, and very strong Emsian quartzitic sandstone (Text-fig. 3). The strongest rocks in the HCM are Cambrian quartzitic sandstones from the Łysogóry Unit, in direct contact with the Kielce Unit on the south. These rocks are similar in mechanical properties to part of the sandstones in a narrow belt in the Dyminy Anticline (Text-figs 1b, 3).

Mechanical stratigraphy controls the geometry of multilayer folds (e.g. RAMSAY 1974; FISHER & JACKSON 1999; GUTIÉRREZ-ALONSO & GROSS 1999; CHESTER 2003), hence it is necessary to investigate the mechanical properties of rocks. The laboratory-measured mechanical properties of Palaeozoic rocks from the Kielce Unit emphasize the current differences between the individual rock complexes (PINIŃSKA 1994, 1995) (Text-fig. 3). During Variscan deformation the rocks were probably to a large extent fluid-saturated because the youngest of the folded rocks, represented by Viséan deposits, developed as a deepening upward succession with a weakly pronounced regressive tendency (SZULCZEWSKI 1995). Thus, for comparison of the compressive strengths (Rcn), water-saturated samples were studied (PINIŃSKA 1994, 1995).

The data on the Palaeozoic rocks investigated from the Kielce Unit indicate current compressive strengths ranging from 51 to 98 MPa, tensile strengths (T) from 5.5 to 18.2 MPa and shear strengths (τ) from 11.8 to 19.1 MPa (PINIŃSKA 1994) (Text-fig. 3). The compressive strengths of the quartzitic sandstones have not been investigated (PINIŃSKA 1994), but their strengths can probably distinctly exceed 100 MPa.

The oldest rocks exposed in the study area are Lower and Middle Cambrian shale alternating with thin-bedded, fine-grained sandstone and sandstone with intercalations of conglomerate (Text-fig. 3) (e.g. ORŁOWSKI 1975). This rock complex is generally incompetent, apart from the Lower/Middle Cambrian quartzitic sandstones in the hinge of the Dyminy Anticline, which were not laboratory tested (Text-fig. 1b). In comparison, the mechanical properties of the Upper Cambrian quartzitic sandstone in the southern part of the Łysogóry Unit (Wiśniówka Quarry) include extremely high tensile strength (T) ranging from 16.7 to 20.0 MPa, shear strength from 31.0 to 44.7 MPa and compressive strength from 56 to 275 MPa (PINIŃSKA 1994). Above the Middle Cambrian/Ordovician unconformity in the Kielce Unit, Ordovician and Silurian rocks comprise conglomerate, limestone, mudstone, shale and greywacke. The laboratory tested Ordovician limestones (Mójcza Quarry) are more competent than the weaker part of the Cambrian rocks. T is equal to 7.1 MPa and τ and Rcn range from 13.9 to 17.5 MPa, and from 51.0 to 89 MPa, respectively (PINIŃSKA 1994) (Text-fig. 3). The Lower Devonian rock sequence consists of sporadically occurring Gedinian-Ziegenian conglomerate and Emsian quartzitic sandstone with intercalations of shale (TARNOWSKA 1981; SZULCZEWSKI 1995). This rock complex is similarly competent to the higher carbonate rock complex. High strength parameters also have been observed in the Emsian sandstone (Text-fig. 3, Barcza Quarry) (PINIŃSKA 1994) in both the Łysogóry and Kielce units (e.g. SZULCZEWSKI 1995). The values of T and τ for Emsian sandstone are 11.8-18.2 MPa and 11.9-32.0 MPa, respectively (PINIŃSKA 1994, 1995) (Text-fig. 3). The overlying Middle-Upper Devonian sequence consists mainly of carbonates. Dolostone forms the lower part of this complex (generally Eifelian and lower Givetian). Shale and limestone prevail above,

Fig. 2 a – Simplified tectonic sketch-map of the HCM with investigated and cited quarries*: 1 – Laskowa, 2 – Kostomłoty, 3 – Mogiłki, 4 – Barcza, 5 – Wiśniówka, 6 – Śluchowice, 7 – Jaworznia, 8 – Szewce, 9 – Ostrówka, 10 – Stokówka, 11 – Zelejowa, 12 – Zamkowa, 13 – Jaźwica, 14 – Radkowice, 15 – Kowala-Nowiny II, 16 – Trzuskawica, 17 – Sitkówka-Nowiny (Zgórsko), 18 – Łabędziów, 19 – Słopiec, 20 – Mójcza, 21 – Józefka, 22 – Górno, 23 – Winna, 24 – Wszachów, 25 – Piskrzyn, 26 – Wymysłów, 27 – Karwów, 28 – Jurkowice Budy. b – Tectonic sub-units in the Kielce Unit. For other explanations see Fig. 1 and the text

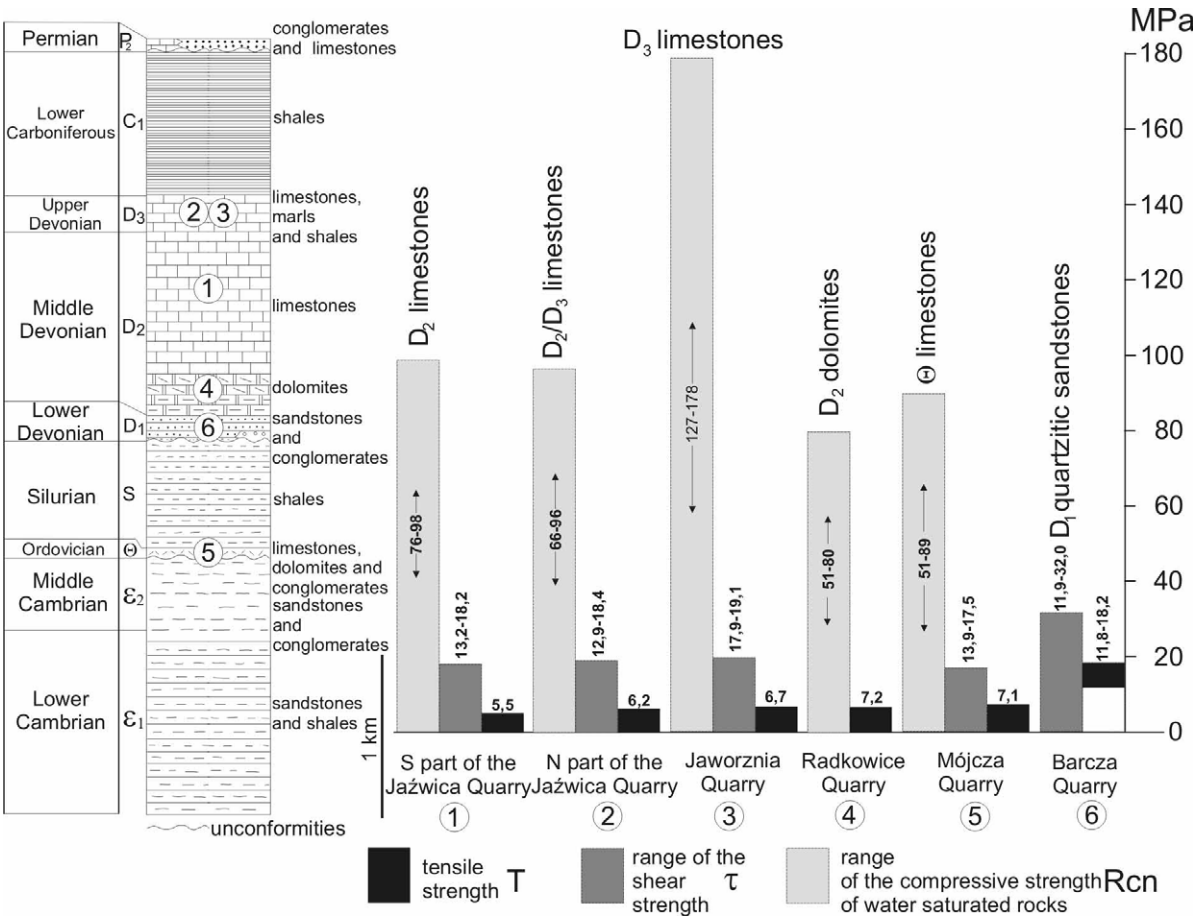

Fig. 3. Lithostratigraphic columns of strata from the southern part of the Holy Cross Mountains. (based on HAKENBERG 1974; ORŁOWSKI 1975; HAKENBERG & *al.* 1976; STUPNICKA 1992 – and references cited therein) with current selected mechanical parameters of rocks (PINIŃSKA 1994). For other explanations see text

up to the Fammenian. In the Devonian carbonate rocks, the highest values of T are in Eifelian and Givetian dolomites, up to 7.2 MPa (PINIŃSKA 1994, 1995) (Text-fig. 3, Radkowice Quarry). The Middle/Upper Devonian limestone above them is slightly weaker in tensile strength. The T, τ and Rcn range from 5.5 to 6.7 MPa, from 13.2 to 19.1 MPa and from 76 to 178 MPa, respectively (Text-fig. 3, Jaźwica and Jaworznia quarries). Above the Devonian rocks, an incompetent Carboniferous rock complex comprising siliceous shales with radiolarites and siderites was not laboratory tested.

FOLDS AND MESOSTRUCTURES

Map-scale folds

Folds within fault-bounded block domains

The HCM fold belt in the Kielce Unit consists of series of map-scale folds, formed of Lower Cambrian to Lower Carboniferous rocks (CZARNOCKI 1938), exposed in a fold belt, up to 160 km long and 15-20 km wide (Text-figs 1b and 2b). The Kielce Unit is divided traditionally into the Kielce-

Fig. 4. a – Geological cross-section (A-B-C) through the Kielce Unit based on FILONOWICZ (1973a) and HAKENBERG (1973), slightly modified. Black rectangles – quarries on the limbs of folds, close to the cross-section. $\mathcal{E}_1$ – Lower Cambrian, $\mathcal{E}_2$ – Middle Cambrian, D_1 – Lower Devonian, D_2 – Middle Devonian, D_3 – Upper Devonian, C_1 – Lower Carboniferous, P_3 – Upper Permian, T_1 – Lower Triassic, T_2 – Middle Triassic, T_3 – Upper Triassic, J_1 – Lower Jurassic, J_2 – Middle Jurassic, J_3 – Upper Jurassic. For location of cross-section and other stratigraphic information see Fig. 1b. b – Folds on western wall of the Śluchowice Quarry. c – Shaded relief image created from digital elevation model from the Niewachlów Anticline area with fold axial traces and thrust fault marked. d – Geological cross-section through the Niewachlów Anticline based on CZARNOCKI (1956, his pl. 22), slightly modified. For location of cross-section and other stratigraphic information see Fig. 1b. e – Chevron folds in the Mogiłki Quarry. The folds consist of Frasnian thin-bedded limestone and shale. Average bed thickness is 15 cm. Location of the quarries presented on Fig. 2a. For other explanations see text

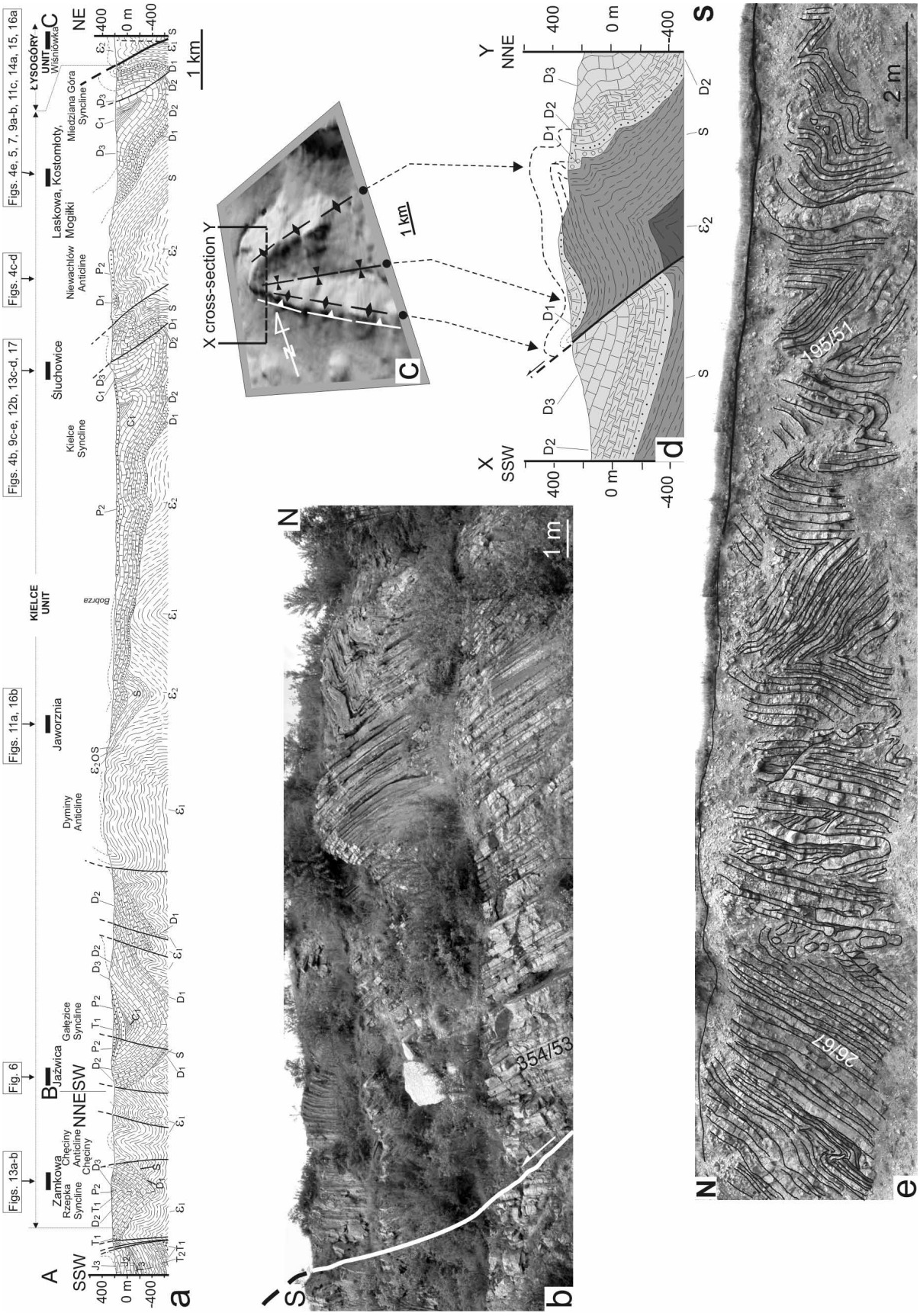
Figs. 13a-b
Fig. 6
Figs. 11a, 16b
Figs. 4b, 9c-e, 12b, 13c-d, 17
Figs. 4c-d
Figs. 4e, 5, 7, 9a-b, 11c, 14a, 15, 16a
KIELCE UNIT
ŁYSOGÓRY UNIT
Zamkowa Rzepka Syncline
Checiny Anticline
Jaworznia
Jaźwica
Galęzice Syncline
Dyminy Anticline
Bobrza
Kielce Syncline
Ślichowice
Niewachlów Anticline
Laskowa, Kostomłoty, Miedziana Góra Syncline
Wiśniówka
SSW
NNE
NE
1 km
0 m
400
-400
a
b
c
d
e
X cross-section Y
X
Y
SSW
NNE
N
S
1 m
2 m
354/53
195/51
26/67

Łagów Synclinorium and the Chęciny-Klimontów Anticlinorium (SAMSONOWICZ 1926; ZNOSKO 1962) (Text-figs 1b and 2b), where the folds are dissected by numerous, longitudinal faults parallel to the fold axes and cross-fold faults (CZARNOCKI 1919, 1938, 1961a–f; SAMSONOWICZ 1934). In this study, the faults were identified from strike separations and rotations of bedding observed during the field investigations and interpreted using radar images and DEM analyses (e.g. KONON & ŚMIGIELSKI 2006). The dip-slip component was commonly observed along the faults, but the strike-slip component, was more difficult to assess. The longitudinal faults, *sensu* TWISS & MOORES (1992), were thrusts or in some places reverse faults. They dissect mainly the forelimbs of asymmetric folds and both limbs of symmetric folds (Text-figs 4a, c and d) (e.g. CZARNOCKI 1956, pl. 12; BEDNARCZYK & *al.* 1970; KOWALSKI 1975; MIZERSKI 1995, fig. 17; ORŁOWSKI & MIZERSKI 1995, fig. 4).

The Kielce Unit is divided along the first-order faults into smaller fault-bounded block domains (Text-fig. 2b). In the zones between the individual block domains, the trends of the fold axes change even in the range of tens of degrees (Text-fig. 1b). The possibility of separation into smaller tectonic sub-units for the northern part of the Kielce-Łagów Synclinorium was suggested earlier by SAMSONOWICZ (1926). The presence of block domains that were displaced in relation to each other were also suggested by KOWALCZEWSKI (1971) for the Kielce and Łysogóry units.

Kielce-Łagów Synclinorium

Based on CZARNOCKI's studies (1938, 1957, 1961a, b, d, e, f), the Kielce-Łagów Synclinorium can be divided into two longitudinal zones – northern (I) and southern (II) (Text-figs 1b and 2b). The northern (I) zone is bordered on the north by the Holy Cross Fault and on the south by 105-125° striking longitudinal faults (CZARNOCKI 1938, 1957, 1961a, b, d, e, f): the Niewachlów Fault (NF) (CZARNOCKI 1957) and two other faults referred to as the Bieliny Kapitulne Fault (BkF) and Janczyce Fault (JaF) (Text-figs 1b and 2b). This zone is also cut by transverse faults including the Oziębłów Fault (OF) and two faults referred to as the Porąbka Fault (PF) and Łagów-Michałów Fault (Ł-MF) (Text-fig. 1b). These folds and the HCF divide the northern zone into three smaller fault-bounded block domains (Ia, Ib and Ic) (Text-figs 1b and 2b).

In the northern zone (I), within block Ia, eastward to the Porąbka Fault, first-order folds are from a few to tens of kilometres long and include the Niewachlów Anticline (N a.), the Miedziana Góra Syncline (MG s.) and two second-order folds – the Miedziana Góra Anticline (MG a.) and Bukowa Anticline (Bk a.) (CZARNOCKI 1938, FILONOWICZ 1973a, b) (Text-figs 1b and 2b). Within block Ib between the Porąbka and Łagów-Michałów Faults there are the Bieliny Anticline (Bl a.), which probably continues eastward as the Małacentów Anticline (Mł a.), the Bartoszowiny Syncline (Ba s.) and two second-order folds – the Płucki Syncline (Pł s.) and Płucki Anticline (Pł a.) (CZARNOCKI 1929b, 1961b; WALCZOWSKI 1966, 1968). Within the easternmost block Ic there are the Sobiekurów-Grocholice Syncline (Sb-G s.), Baćkowice Anticline (Bc s.), Żerniki-Karwów Syncline (Ż-K s.), Ublinek Anticline (Ub a.) and the Międzygórz Syncline (Md s.) (SAMSONOWICZ 1934; CZARNOCKI 1961b, c, e, f; WALCZOWSKI 1966, 1968; DOWGIAŁŁO 1974a, b).

The southern zone (II) of the Kielce-Łagów Synclinorium is in direct contact with the Chęciny-Klimontów Anticlinorium on the south (Text-figs 1b and 2b). Similarly to the northern (I) zone, the southern II zone comprises fault-bounded block domains (IIa, IIb, IIc and IId) (Text-fig 2b). Block IIa is bordered on the east by faults which probably constitute the northern part of the Mójcza Fault Zone (MFZ). Block IIb is bounded by the MFZ on the west and by the Porąbka Fault on the east, respectively (Text-figs 1b and 2b). Block IIc continues eastward to the Łagów-Michałów Fault (Ł-MF). East of this fault is the IId block. The southern zone includes the Kielce Syncline (K s.), the Kielce Anticline (K a.), the Radlin Syncline (R s.), the Łagów Syncline (Łg s.), the Piotrów Syncline (P. s.), the Ujazd Syncline (U s.) and the Kabza Anticline (Kb a.) (Text-figs 1b and 2b).

Chęciny-Klimontów Anticlinorium

The southern part of the Kielce unit is the Chęciny-Klimontów Anticlinorium, which is divided into at least four block domains bounded by transverse fault zones (Text-figs 1b and 2b). The first (IIIa), westernmost block is between the Mesozoic margin and the Mójcza Fault Zone

(MFZ); the second (IIIb) is between the MFZ and the Łukawki Fault (MIZERSKI & ORŁOWSKI 1993) (ŁkF); the third (IIIc) is between the ŁkF and the Łagów-Michałów Fault (Ł-MF) and the fourth (IIId) is east of the Ł-MF (Text-figs 1b and 2b).

From the south within block IIIa there are the Zbrza Anticline (Zb a.), the Chęciny Anticline (Ch a.), the Gałęzice-Bolechowice Syncline (G-B s.) and the Dyminy Anticline (D a.) (Text-figs 1b and 2b). East from the Mójcza Fault Zone (MFZ) and from the south within block IIIb there are the Łabędziów Anticline (Ł a.), the Łabędziów Syncline (Ł s.), the Komórki Anticline (Km a.), the Gałęzice-Bolechowice Syncline (G-B s.), the Daleszyce Anticline (Dl a.), the Daleszyce Syncline (Dl s.) and the Niestachów Anticline (Ns a.), which passes eastward into the Orłowiny Anticline (O a.) (Text-figs 1b and 2b). Within block IIIc first-order folds include the Ociesęki Anticline (Oc a.), the Bardo Syncline (Bd s.) and the Orłowiny Anticline (O a.). These folds probably continue within the most eastern block IIId where the Orłowiny Anticline (O a.) and Bardo Syncline may pass into the Radwan Anticline (R a.) and Wygiełzów Syncline (Wg s.), respectively. Within the block east of the Samotnia-Oziębłów Fault are the Łownica Anticline (Łw a.), Beradz Syncline (Br s.), Nawodzice Syncline (Nw s.) and at least a few folds near Klimontów (ROMANEK 1977) (Text-figs 1b and 2b).

Geometry of folds

The folds in the Kielce Unit exhibit distinct variations in wavelengths, in the range of 1.5-8 km (Text-fig. 3a). The amplitudes range from 0.2 to 0.8 km. The folds trend generally 95-120°, but in some places between individual block domains, the trends change distinctly and folds display sigmoidal shapes on the geological maps (Text-fig 1b). The Daleszyce Syncline, which passes eastward into the Bardo Syncline (CZARNOCKI 1957), generally trends 105° in the IIIb block, 147° between blocks IIIb and IIIc, and 105° again in the Bardo region (Text-fig 1b). A similar change of trend occurs between Kielce and Daleszyce, where the Kielce Syncline in the Mójcza Fault Zone (MFZ) region passes probably into the Daleszyce Syncline, according to CZARNOCKI's map (1938) and FILONOWICZ (1973a, b; 1976a, b) (Text-fig 1b). The folds in the Kielce Unit display different shape profiles. They are symmetric as well as asymmetric folds (e.g. Text-fig. 4). The hinge zones of the folds in the Kielce Unit commonly comprise a few second-order anticlines and synclines (e.g. Text-fig. 4a) (CZARNOCKI 1938, 1961a–f). These structures were observed in detail by many authors in the hinge zones e.g. of the Chęciny Anticline (CZARNOCKI 1956, his pl. 21; STUPNICKA 1986), the Niewachlów Anticline (CZARNOCKI 1956, his pl. 12), the Dyminy Anticline (FILONOWICZ 1973a, 1973b) or in the Orłowiny Anticline (KOWALCZEWSKI & RUBINOWSKI 1962, fig. 4).

The geometries of the fold shape profiles also commonly change along their axes. For example, these changes are clearly visible in the Niewachlów and Chęciny anticlines. The geometry of the Niewachlów Anticline varies from the west, where the fold has an asymmetric geometry (FILONOWICZ 1973a; LAMARCHE & *al*. 1999, fig. 3) to the east, where a fan-shape geometry prevails (Text-figs 4a and d) (e.g. CZARNOCKI 1956, pl. 12, 1957; KONON & ŚMIGIELSKI 2006). Similarly, the Chęciny Anticline in the westernmost part is south-vergent and has an asymmetric geometry (CZARNOCKI 1929a; KUTEK & GŁAZEK 1972; KOWALSKI 1975; DĘBOWSKA 2004), whereas a symmetric geometry prevails in its eastern part (CZARNOCKI 1956, pl. 21; KUTEK & GŁAZEK 1972; HAKENBERG 1973; KOWALSKI 1975). According to FILONOWICZ (1967, 1968), this anticline has a fan-shape geometry about 6 km east of Chęciny. Further to the east, the hinge zone of the first-order fold divides into two anticlinal branches – the Komórki and Łabędziów anticlines (FILONOWICZ 1967, 1968).

Mesoscopic folds

Mesoscopic folds with small wavelengths in the range of 0.7-9 m are common on the limbs of the map-scale folds (e.g. Text-figs 4b, e, 5, 6 and 7; Tab. 1). These folds trend mostly similarly as the map-scale folds (Text-fig. 8 – I group of the fold axes). Secondary minor folds (Text-fig. 8 – II group of the fold axes) (RACKI & ZAPAŚNIK 1979) have also been observed in the upper parts of the main folds from the Jaźwica Quarry. The axial planes are generally steeply dipping (>75°) (e.g. Text-figs 4e, 5 and 7), although shallowly dipping axial planes (0-40°) also occur (e.g. Text-figs. 4b and 6a-b). The interlimb angles vary strongly, with prevailing angles at 50-60° (Tab. 1). Most of the investigated upright as well as overturned mesoscopic folds consist of thin-

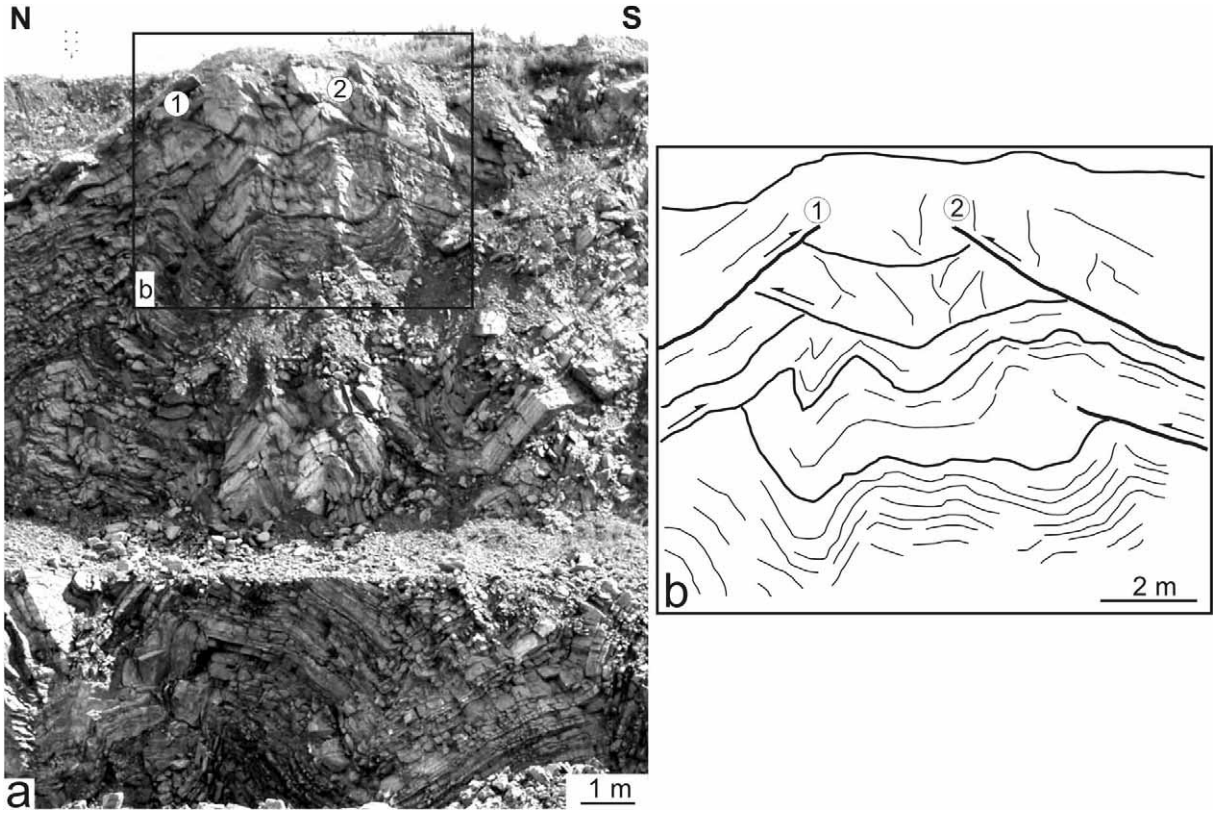

Fig. 5. a – Symmetric folds in the eastern wall of the Kostomłoty Quarry. The folds consist of Frasnian thin-bedded limestone and shale. b – Enlarged part with movement horizons marked. For location of quarry see Figs 2a and 4a

bedded limestone, marl and shale and commonly have chevron profiles (Text-figs 4e, 5, 9a-b). These mesoscopic folds are both symmetric and asymmetric (e.g. Text-figs 4b, e, 5a, 6 and 7). Commonly, thickening of shale, marl and limestone was observed in the fold hinges (e.g. Text-figs 4e and 9c). In the thick layers, bulbous hinge structures (RAMSAY 1974) also occur (Text-figs 9c and d).

Quarry	Figure	Rock type	Wavelength/2 L/2 [m]	Amplitude A [m]	Interlimb angle α
Mogiłki	Text-fig. 4e	thin-bedded limestone and shale	1.5 1.6 0.7 1.7 1.6 1.3	1.1 1.1 1.1 1.1 1.1 1.1	60° 58° 20° 45° 60° 48°
Kostomłoty	Text-fig. 5	thin-bedded limestone and shale	1.3 2.9 1.4 1.6 1	0.7 2.1 1.7 0.7 0.4	60° 80° 57° 85° 85°
	Text-fig. 9a		1.4	1	55°
Jaźwica	Text-fig. 6a	thin-bedded limestone and shale	9	8	55°
Śluchowice	Text-fig. 9c	thin- to medium-bedded limestone and marly shale	3.7	2.6	65-75°

Table 1. Comparison of the geometric and stratigraphic characteristics of mesofolds discussed in the text

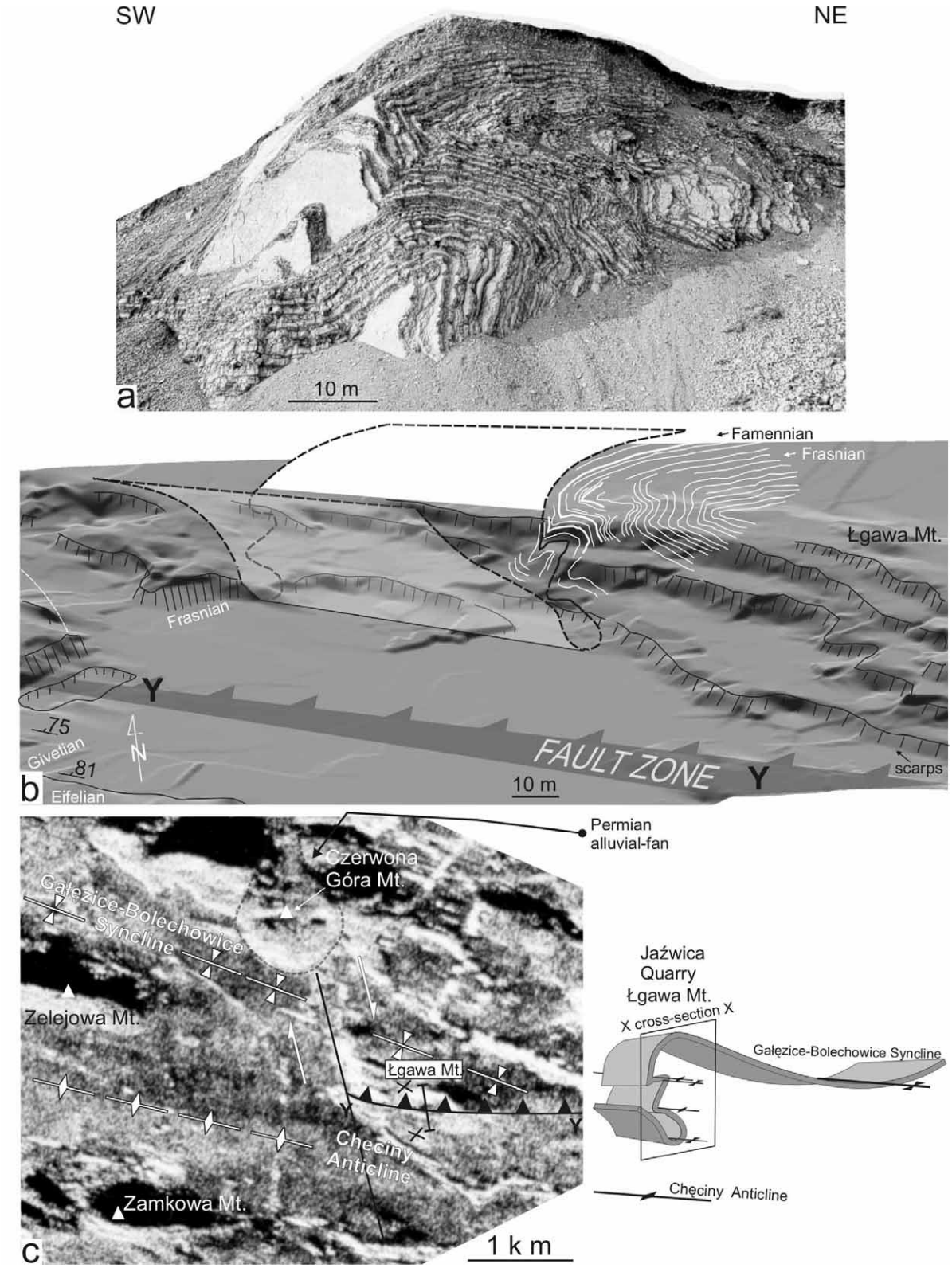

Fig. 6. a – Recumbent folds in the Jaźwica Quarry (photographed by B. A. MATYJA about 1982). The folds consist of Upper Devonian thin-bedded limestone and shale. Average bed thickness is 10 cm. b – Reconstructed folds with marked fault zone on the digital elevation model of the quarry as the background. c – Tectonic sketch on the radar image as the background with 3D-view sketch of folds in the eastern block of a strike-slip fault. For location of quarry see Figs 2a and 4a. For other explanations see text

In addition to the typical chevron folds, box-shaped folds (e.g. Text-fig. 6a) and m-fold are characterized by the occurrence of second-order anticlines with subsidiary synclines in the hinge zones of first-order folds (e.g. Text-fig. 5).

Typical symmetric chevron folds (Text-figs 4b and 4e – central and northern portion of the Mogiłki Quarry) and slightly asymmetric folds comprising thick-bedded limestones gently rounded in the upper portion of the hinge and intensively folded downwards can co-occur at the same quarry level (Text-figs 4b and 4e – southern part of the Mogiłki Quarry). Some of the overturned and recumbent mesoscopic folds occur on short limbs of large map-scale asymmetric folds (Text-figs 4a-b, 9c). In some places significant decrease of bed thickness in the forelimbs in comparison to the backlimbs has also been observed in the overturned and recumbent asymmetric folds.

Some of the mesoscopic folds which developed on the limbs of the map-scale folds occur near the cross-fold faults (CZARNOCKI 1938, 1956, pl. 22) (e.g. Text-figs 6 and 7). For example, groups of folds from the southern limb of the Gałęzice-Bolechowice Syncline and from the southern limb of the Miedziana Góra Syncline occur only in the eastern fault blocks of these faults. In both examples, strongly folded layers from the E fault blocks (e.g. Text-figs 5 and 6) contrast with slightly folded layers occurring in the W fault blocks (e.g. Text-fig. 6).

Mesostructures in the folds

Multilayer folds display numerous mesofaults, cleavage, and additionally, somewhat rarer small-scale thrust duplexes, stylolites and boudinage. These mesostructures developed due to different deformation mechanisms associated with the progressive shape modifications of such folds.

Mesofaults

The limbs and hinge zones of the investigated symmetric and asymmetric folds commonly display

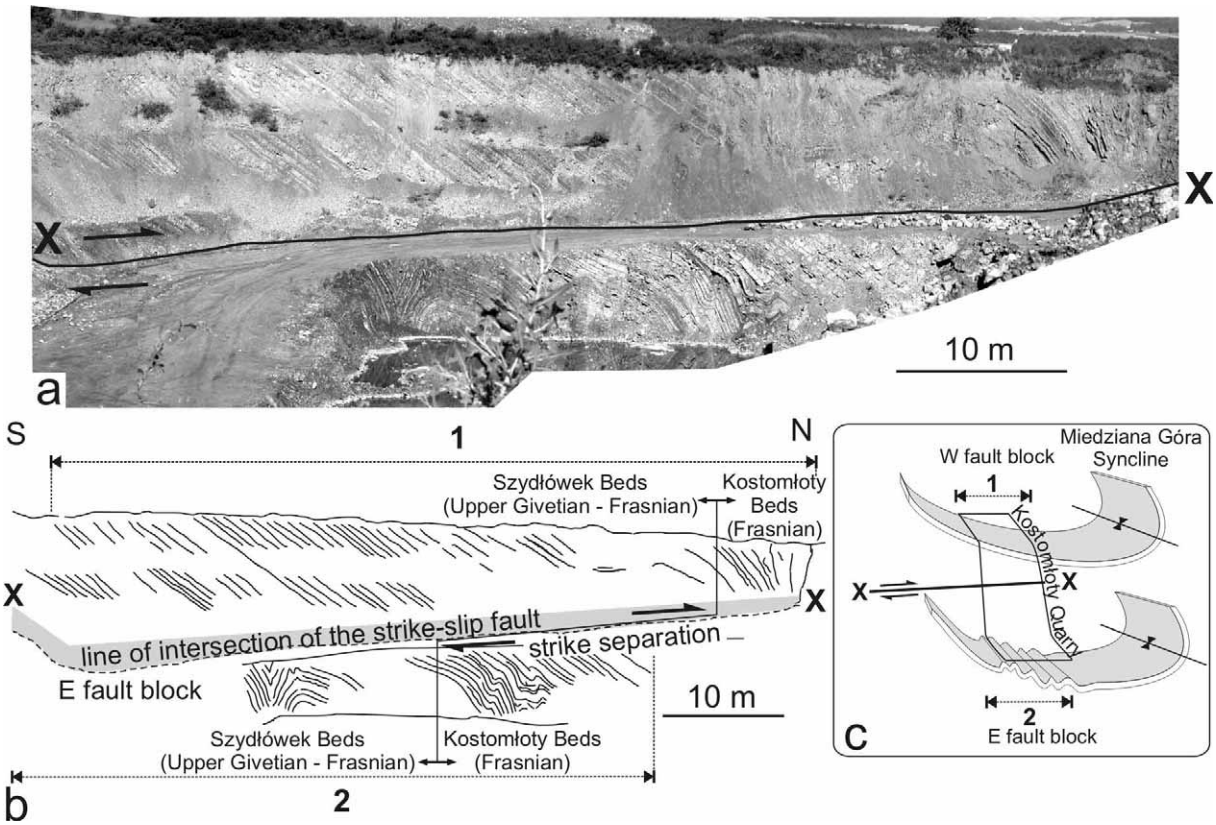

Fig. 7. Folds in the southern limb of the Miedziana Góra Syncline. a – Dextral strike-slip fault in the Kostomłoty Quarry. b – Sketch of both blocks of the dextral strike-slip fault in the western part of the Kostomłoty Quarry. Lithostratigraphic units based on personal communication with M. SZULCZEWSKI in 2005. The folds consist of Frasnian thin-bedded limestone and shale. Average bed thickness is 15 cm. c – Sketch showing the differences in development of both blocks of the strike-slip fault in the Kostomłoty Quarry. For location of quarry see Figs 2a and 4a

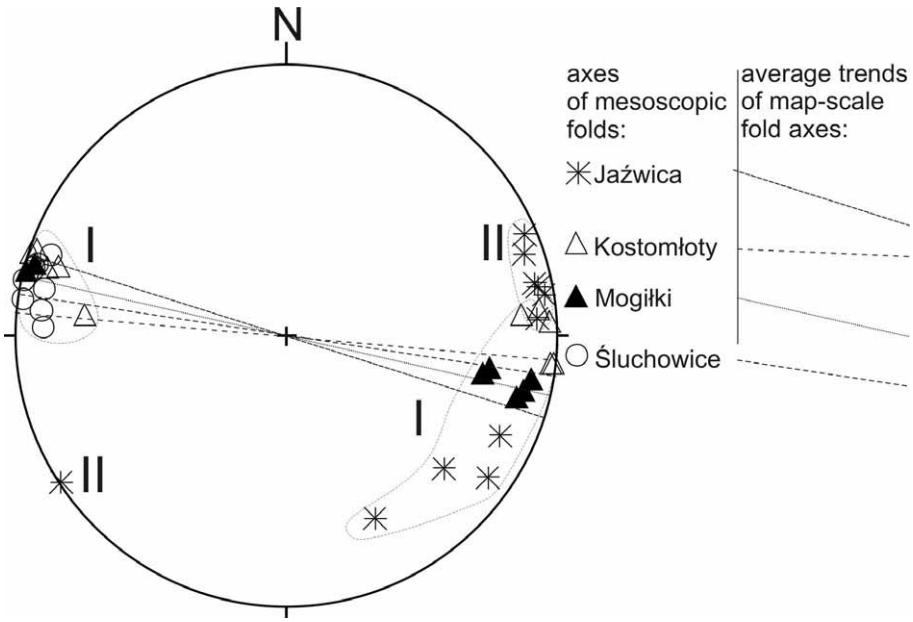

Fig. 8. Diagram of the axes of the mesoscopic folds. I – group of folds with axes sub-parallel to map-scale folds. II – group of folds from the Jaźwica Quarry with axes different from the map-scale folds

cm-displacement dip-slip faults, which dissect only a few layers. These faults strike generally parallel to the fold axes (Text-fig. 10), similarly to those described by HANCOCK & ATIYA (1979, *h0l* faults group – their figs 5f, g) and HANCOCK (1985, figs 17k and l). These faults are symmetrically or slightly asymmetrically orientated about axes parallel to dip directions or normal to the layers. According to HANCOCK & ATIYA (1979), the senses of displacements along the cm-displacement mesofaults relative to the horizontal depend on the inclination of the layer or few layers in which the faults are contained. Hence, in this study such mesofaults were classified according to the terminology of NORRIS (1958) and HANCOCK & ATIYA (1979) as contraction faults when they shorten layers parallel to the dip line and as extension faults when they extend layers parallel to this line. The faults, recognized as typical fold-accommodation faults were classified according to the terminology of MITRA (2002a).

Contraction faults on the fold limbs

Contraction faults comprise conjugate fault systems as well as single sets (Text-figs. 10a, c, e, i-k). Conjugate fault sets prevail on fold limbs, dipping up to about 60°. Single fault sets occur instead on the steeper limbs. The fault sets are symmetrically (e.g. Text-figs 11a, c, F_1-F_2 sets) as well as distinctly asymmetrically (e.g. Text-figs. 11b, F_1'-F_2' sets) orientated about the axis parallel to the dip line (HANCOCK & ATIYA, 1979, figs 4 and 5). When these fault sets are on fold limbs dipping up to 10-20°, they generally enclose acute dihedral angles (2Θ) up to 45° (e.g. Text-fig. 11a). On folds limbs dipping over 20°, as well as on both limbs of the symmetric and generally short limbs of the asymmetric folds, faults prevail that enclose acute dihedral angles (2Θ) over 50° (e.g. Text-figs 11b, c).

These fault sets develop frequently as structures with ramp-flat geometry when the rock sequences comprise alternating competent and incompetent rocks (Text-figs 11b, c). The asymmetrical orientation of the F_1'-F_2' sets (Text-fig. 11b) about the dip line resulted in the development of a single set (F_2') corresponding to wedge-faults (CLOOS 1961), also referred to as contractional ramps (PEACKOCK & SANDERSON 1992). The second fault set (F_1') is inclined at higher angles (30-50°) to the layering and in contrast to the first fault set, has a tendency to cut a few layers.

Apart from the conjugate sets, single fault sets corresponding to the F_2 set have been observed, particularly on steeply dipping fold limbs (Text-figs 10e, j and 12). They may occur at low as well as high angles to the bedding. On steeply dipping limbs, ramp-flat geometry results when the fault sets cut rock sequences with distinctly different competency (Text-fig. 12a). At the tips of these faults the layers

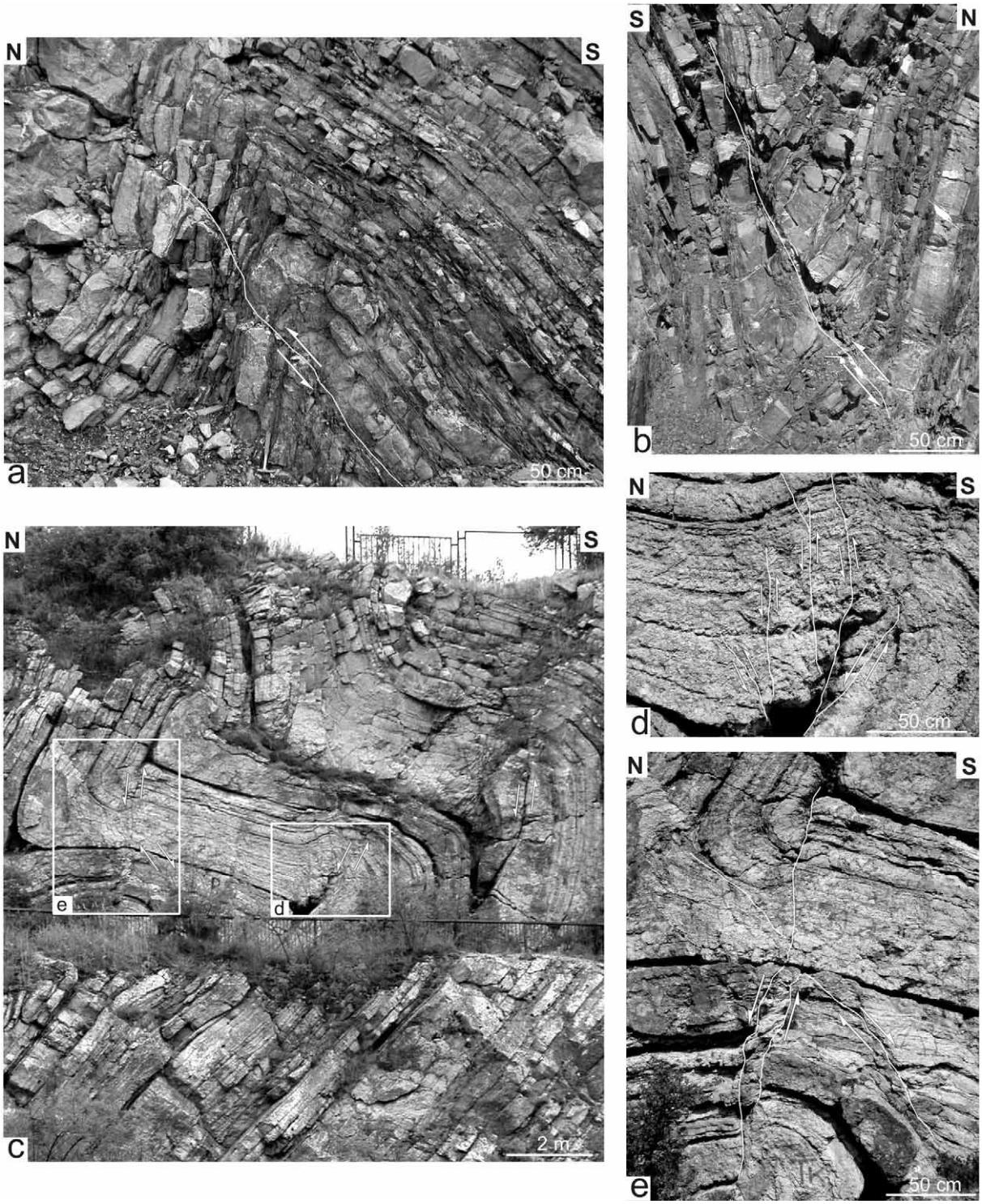

Fig. 9. Examples of fault sets in the hinge zones. a – Into-anticline thrust in the chevron fold in the Kostomłoty Quarry. b – Out-of-syncline thrust in the chevron fold in the Kostomłoty Quarry. c – Folds in the Śluchowice Quarry with marked figures d and e. The folds consist of Frasnian thin- to medium-bedded limestone and marly shale. Average bed thickness is 20 cm. d – Horsetail splays of fractures near the into-anticline thrust in the Śluchowice Quarry. e – Out-of-syncline thrust with the weakly-developed conjugate fault set in the Śluchowice Quarry. For location of quarries see Figs 2a and 4a

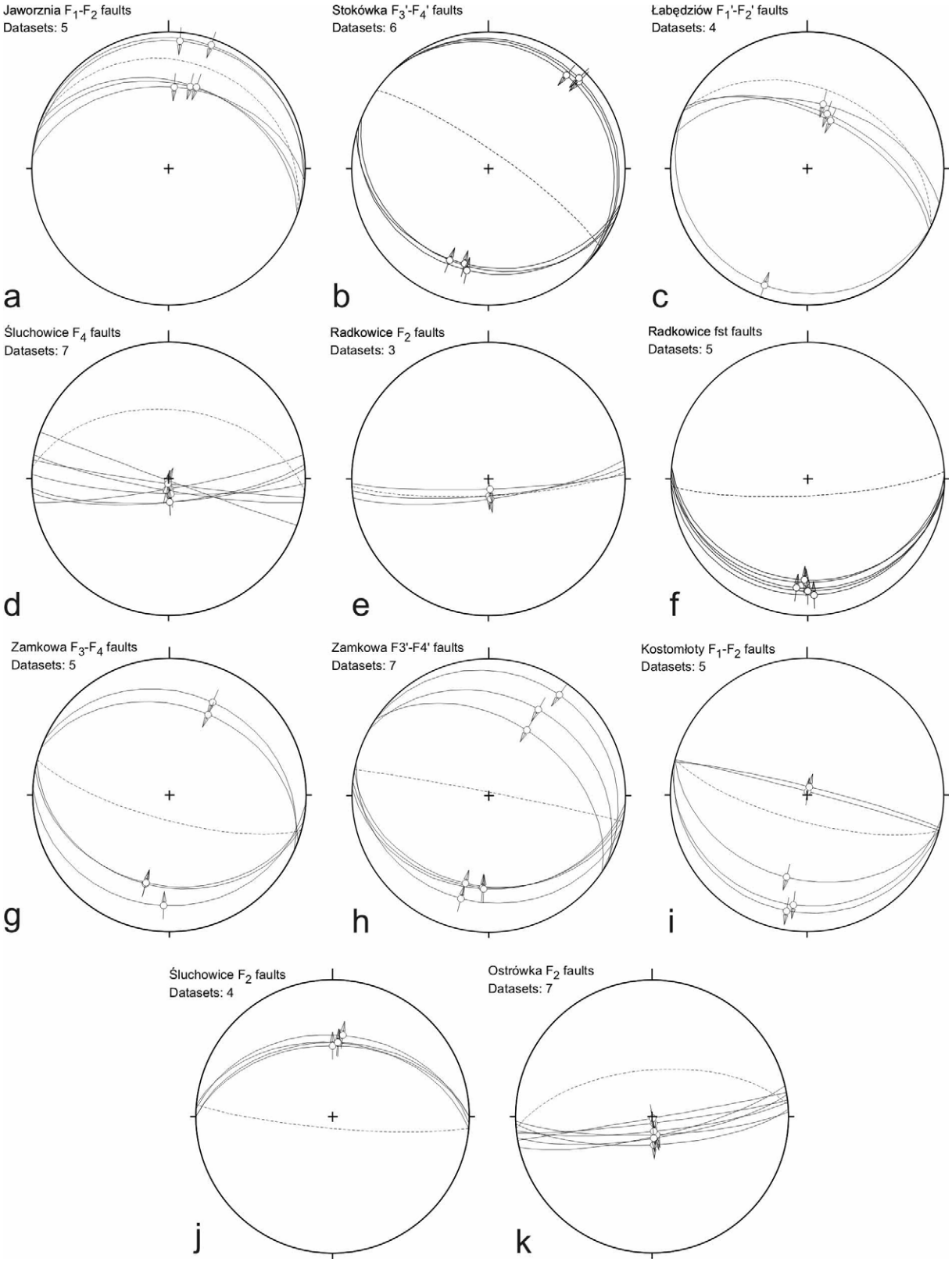

Fig. 10. Examples of diagrams of fault sets occurring on the fold limbs. The average attitudes of the bedding planes marked by dashed lines. For location of quarries see Fig. 2a. For other explanations see text

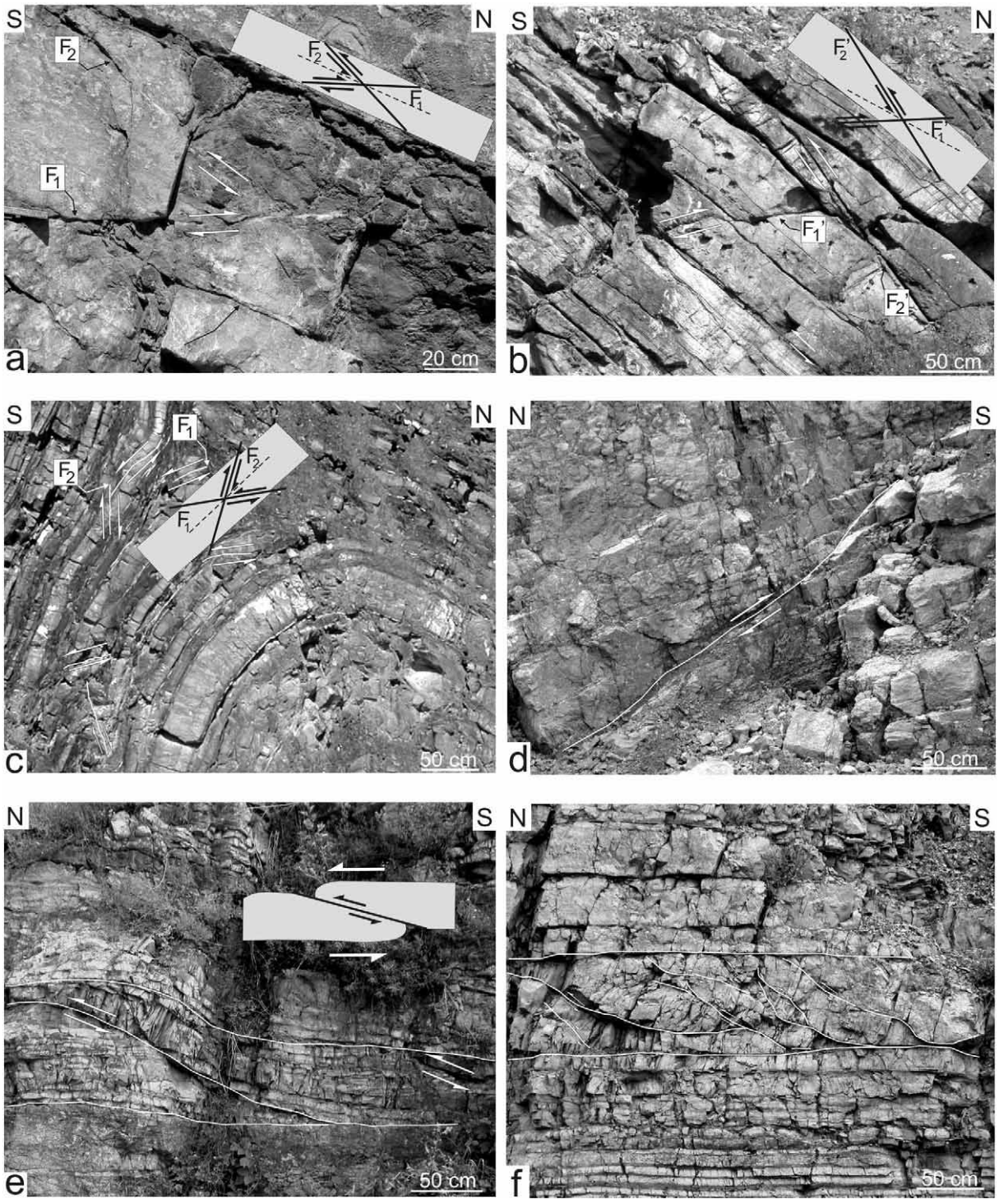

Fig. 11. Examples of contraction fault sets. a – Symmetric F_1-F_2 fault sets in the Jaworznia Quarry. b – Asymmetric F_1'-F_2' fault sets in the Łabędziów Quarry. c – Limb wedge thrusts on the short limb of the asymmetric fold in the Kostomłoty Quarry. d – Wedge thrust at the hinge of the anticline in the Wymysłów Quarry. e – Wedge thrusts in the hinge of the anticline in the Górno Quarry. f – Wedge thrusts forming a cm-scale thrust duplex in the Górno Quarry. For location of quarries see Figs 2a and 4a

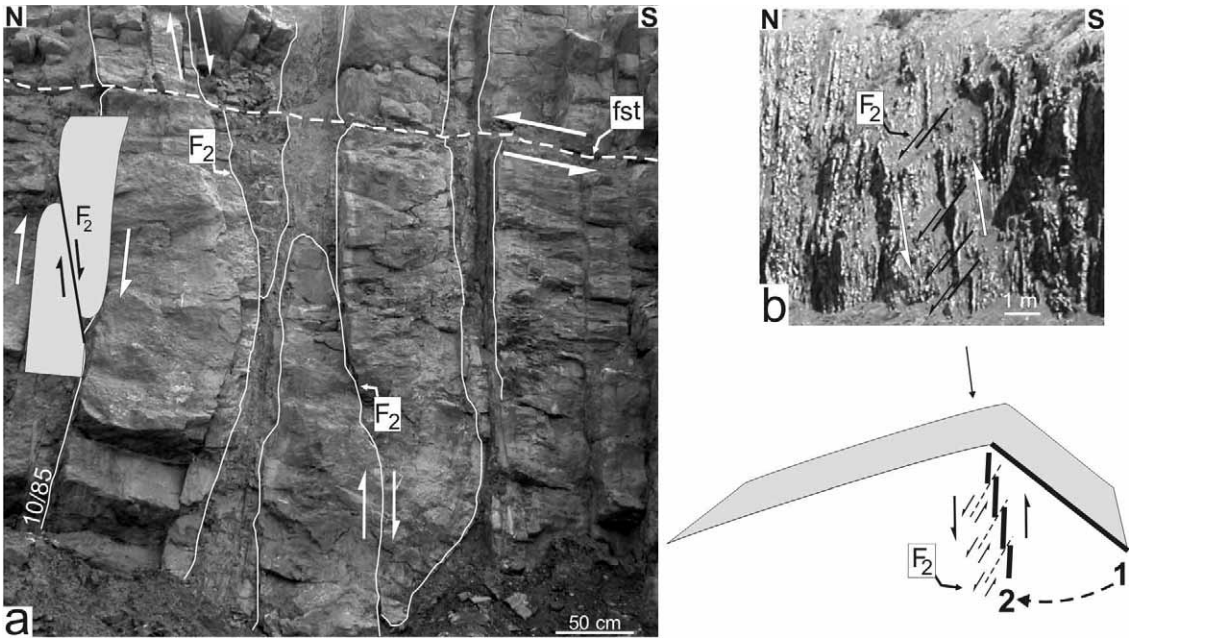

Fig. 12. Examples of fault sets. a – Forelimb shear thrust (fst) and F_2 fault set in the Radkowice Quarry. b – F_2 fault set on the short limb of the Niewachlów Anticline in the Śluchowice Quarry with a sketch suggesting how this set developed. For location of quarries see Figs 2a and 4a. For other explanations see text

are often slightly buckled, which is typical of limb wedge thrusts (MITRA 2002a). In contrast, when they cut layers of similar competency, they are not refracted significantly (e.g. Text-fig. 12b).

Extension faults on the fold limbs

Extension faults, similar to contraction faults, comprise both conjugate and single sets. On the steeply-inclined limbs (>60°), conjugate fault sets comprise faults, which are asymmetrically (Text-figs 10g and 13a, F_3-F_4 sets) and symmetrically (Text-figs 10h and 13b, F_3'-F_4' sets) orientated about the axis perpendicular to bedding (HANCOCK & ATIYA 1979, figs 4 and 5). Apart from these faults, single extension fault sets corresponding to the F_4 set are on overturned fold limbs, inclined generally at high angles to bedding (Text-figs 13c and d).

Faults in hinge zones

Single sets inclined at 60-90° to bedding were noted in the hinge zones of folds with chevron profiles and with the interlimb angles <80° (Text-figs 9a-b and d). These fault sets form thrusts parallel to layering in one of the fold limbs and cut m-thick sequences of rocks in the opposite limb, suggesting that they developed as typical limb thrusts (RAMSAY 1974). According to the terminology introduced by DAHLSTROM (1970) and MITRA (2002a), they correspond to single into-anticline (Text-figs 9a, d) and out-of-syncline thrusts (Text-fig. 9b) (MITRA 2002a). Horsetail splays of fractures are common at the tips of these faults (Text-fig. 9b). The weakly-developed opposite-dipping second fault set, which is conjugate with the into-anticline and out-of-syncline thrusts, was very rarely observed (Text-fig. 9e). Contraction faults, termed as hinge wedge thrusts according to the terminology of MITRA (2002a), also occur at the hinges and probably correspond to the F_1 set (Text-figs 11d and e). In some cases, these form duplexes consisting of many horses (Text-fig. 11f).

Apart from mesofaults dissecting only a few layers, faults also cut m-thick sequences of rock layers or even whole fold limbs. In the Kielce Unit, single sets with features of F_3 and F_3' sets were observed. Some of them cut the F_2 set (e.g. Text-fig. 12a, fst). Similarly to the conjugate sets, they are commonly observed on the short limbs of asymmetrical folds (PRICE 1953 in PRICE & COSGROVE 1990, fig. 15.28). These conjugate fault sets as well as single sets correspond to forelimb shear thrusts (fst) (MITRA 2002a). Faults termed as forelimb space-accommodation thrusts according to MITRA (2002a) also occur in overturned folds (e.g. Text-fig. 4b).

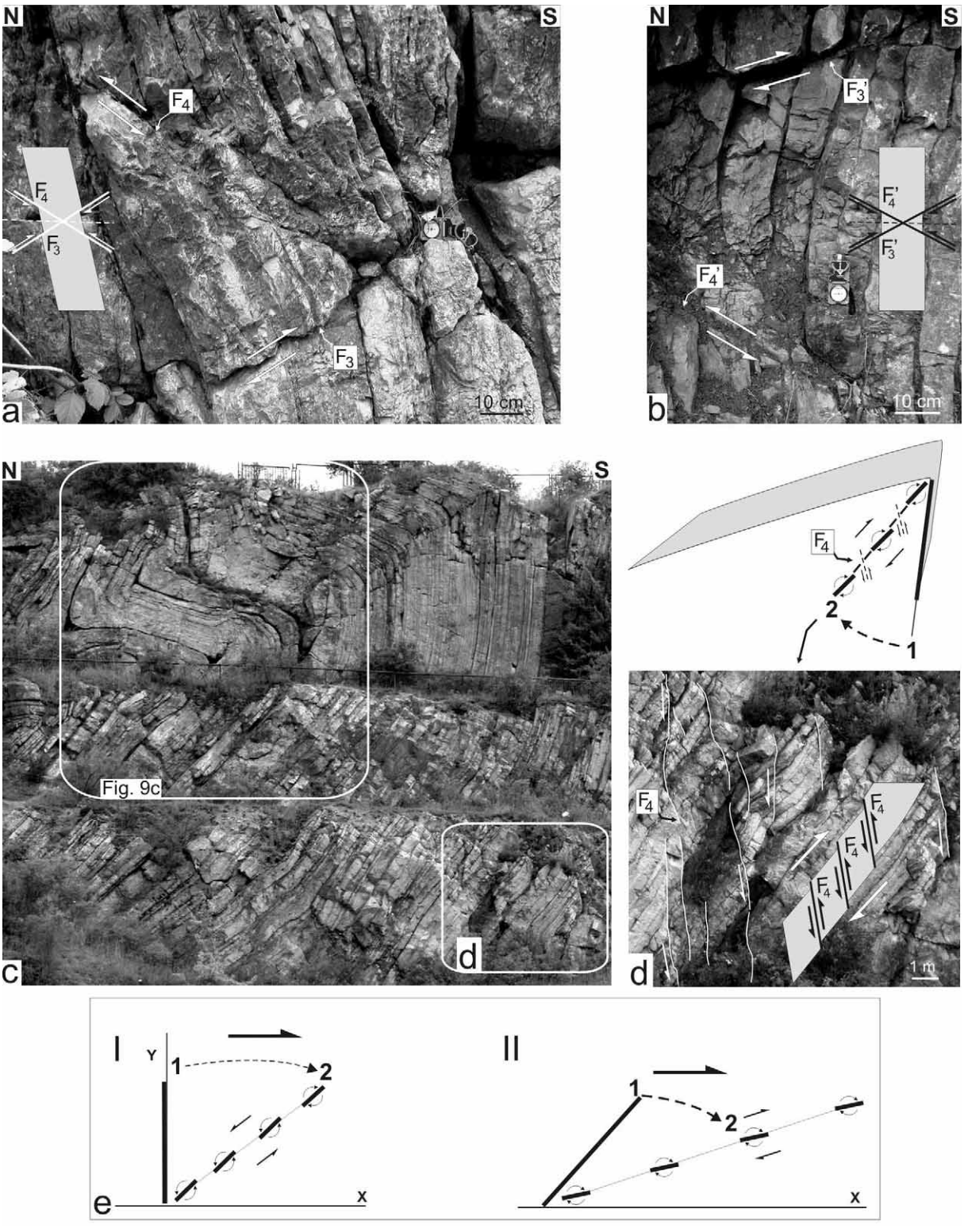

Fig. 13. Examples of extension fault sets. a – Asymmetric F_3-F_4 fault sets in the Zamkowa Quarry. b – Symmetric F_3'-F_4' fault sets in the Zamkowa Quarry. c – Eastern wall of the Śluchowice Quarry with marked figure d. d – F_4 set on the reversed fold limb in the Śluchowice Quarry with a sketch proposing the development of this set. e – Fragmentation of sheets in simple shear, sligthly modified after the model of Ramberg & Ghosh (1977). I – Sheet originally perpendicular to x. II – Angle between sheet and the direction of simple shear below 60°. For location of quarries see Figs 2a and 4a

Cleavage, veins, small-scale thrust duplexes, boudinage and stylolites

Apart from mesofaults, cleavage commonly occurs on the fold limbs (Text-fig. 14). In competent layers this cleavage is spaced at 5-15 cm, but in incompetent layers it is more densely spaced, at 1-5 cm. On the fold limbs with dips ranging from 30 to 60° in rock sequences comprising alternating competent and incompetent layers, the single sets of cleavage are often refracted at the contacts between the layers (e.g. Text-figs 14a and b – Mogiłki and Kostomłoty quarries). On steeply-dipping limbs, two sets of cleavage have also been noted [e.g. Text-figs 14b – Stokówka, Śluchowice (site 1 of quarries)]. These sets have parallel strikes, opposite dips and are commonly linked with arch-like connections suggesting their coeval formation as conjugate sets (e.g. JAROSZEWSKI 1972).

In some quarries, calcite crystal fibres have been observed on the bedding planes. The crystal fibres, which were sampled from the Kostomłoty Quarry, occur in both limbs as well as in the hinge zone of the anticline (Text-fig. 15). The crystal fibres are with wall-rock parallel inclusions resulting from the incorporation of fragments of the wall grains of the carbonate rocks (Text-fig. 15b). The fibres are inclined to bedding and directions of growth of the crystals are convergent to the axial surface of the anticline. The sense of movement during the development of other structures formed in the fibres, such as small blocks rotated in domino style (Text-fig. 15c) and termed, according to COX (1987), as fibre boundary steps (Text-fig. 15e), is consistent with sense interpreted from the growth of crystal fibres (Text-figs 15a, b and d).

Fold limbs display thrust duplexes with a large number of horses and structural thicknesses, ranging from 5 to several tens of cm (Text-fig. 16a). Bed lengths in each horse of these duplexes are up to 1 m. Thrusts of these duplexes generally strike parallel to bedding. The senses of movements interpreted from these contraction duplexes are opposite on both limbs of the same folds.

Apart from these duplexes, stylolites (e.g. Text-fig. 16b) and boudinage (e.g. Text-fig. 17) were observed relatively rarely. The stylolites occur on both limbs of the folds and in the hinge zones. Common stylolitic sets include bedding-parallel lithostatic stylolites with columns sub-perpendicular to bedding. The columns have lengths up to about 1 cm. Apart from these sets, oblique-bed stylolites were also observed (e.g. Text-fig. 16b). The length of columns of the set is from several millimetres to ca. 1 cm. Single-layer boudinage with boudins up to 30 cm, with long axes of boudins striking parallel to the fold axes, occurs mainly on the steeply dipping limbs (Text-fig. 17b).

DISCUSSION

Temperature, pore pressure conditions and compressive stress levels during folding

Palaeotemperatures

The palaeotemperatures in Devonian rocks in the Kielce Unit were investigated based on the colour alteration of conodonts (BELKA 1990) and reflection of vitrinite (MARYNOWSKI 1997). These studies indicate rather low palaeotemperatures – averaging 50-80°C to a maximum of 150°C near the Holy Cross Fault. These temperatures favoured the brittle deformation mechanism.

Pore pressures

Development of folds composed of unmetamorphosed sedimentary layers developed under several km of overburden, suggests that high pore pressures occurred during this folding (e.g. RAMBERG & JOHNSON 1976; PRICE & COSGROVE 1990; COSGROVE 1993). According to PRICE & COSGROVE (1990), during flexural-slip folding initiated under several kilometres of overburden, the ratio (λ) of the pore-fluid pressure relative to the confining pressure could even have exceeded the value 0.95. The possible occurrence of such overpressures in the HCM, according to PRICE & COSGROVE (1990), COSGROVE (1993), and JESSELL & *al.* (1994) is also suggested by calcite crystal fibres observed on the bedding planes (e.g. Text-fig. 15). The opposite sense of movement, interpreted from crystal fibres in both sampled limbs of a fold in the Kostomłoty Quarry shows that they formed during folding when the beds moved over each other according to the flexural-slip mechanism. Additionally, the growth of these fibres suggests that cohesion along the beds was lost due to the occurrence of overpressures, decreasing the resistance to slip between layers (PRICE & COSGROVE 1990).

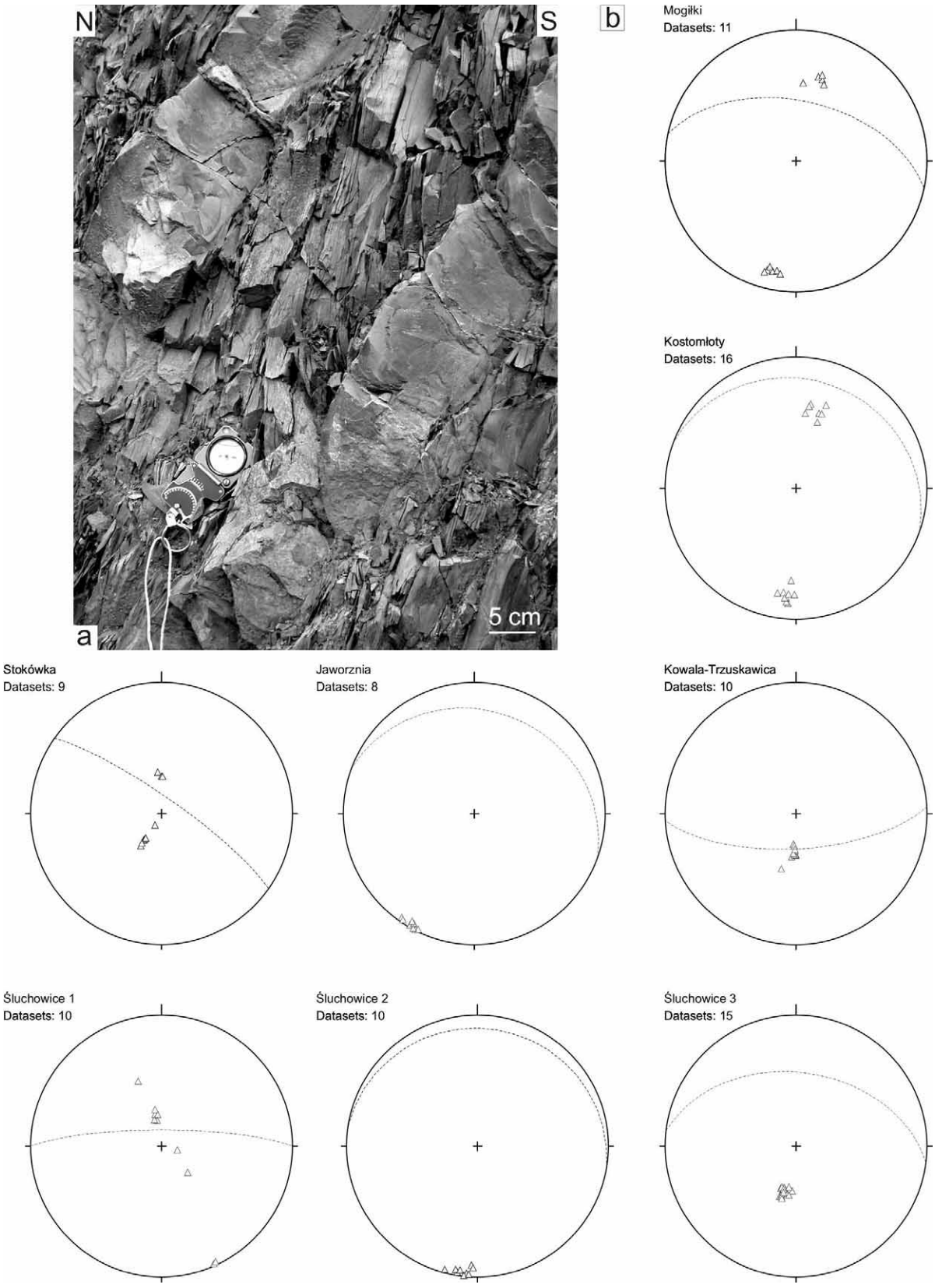

Fig. 14. Examples of cleavage sets. a – Refracted cleavage in the Mogiłki Quarry. b – Examples of diagrams of cleavage sets. Cleavage sets displayed as poles to planes. The average attitudes of the bedding planes marked by dashed lines. For location of quarries see Fig. 2a

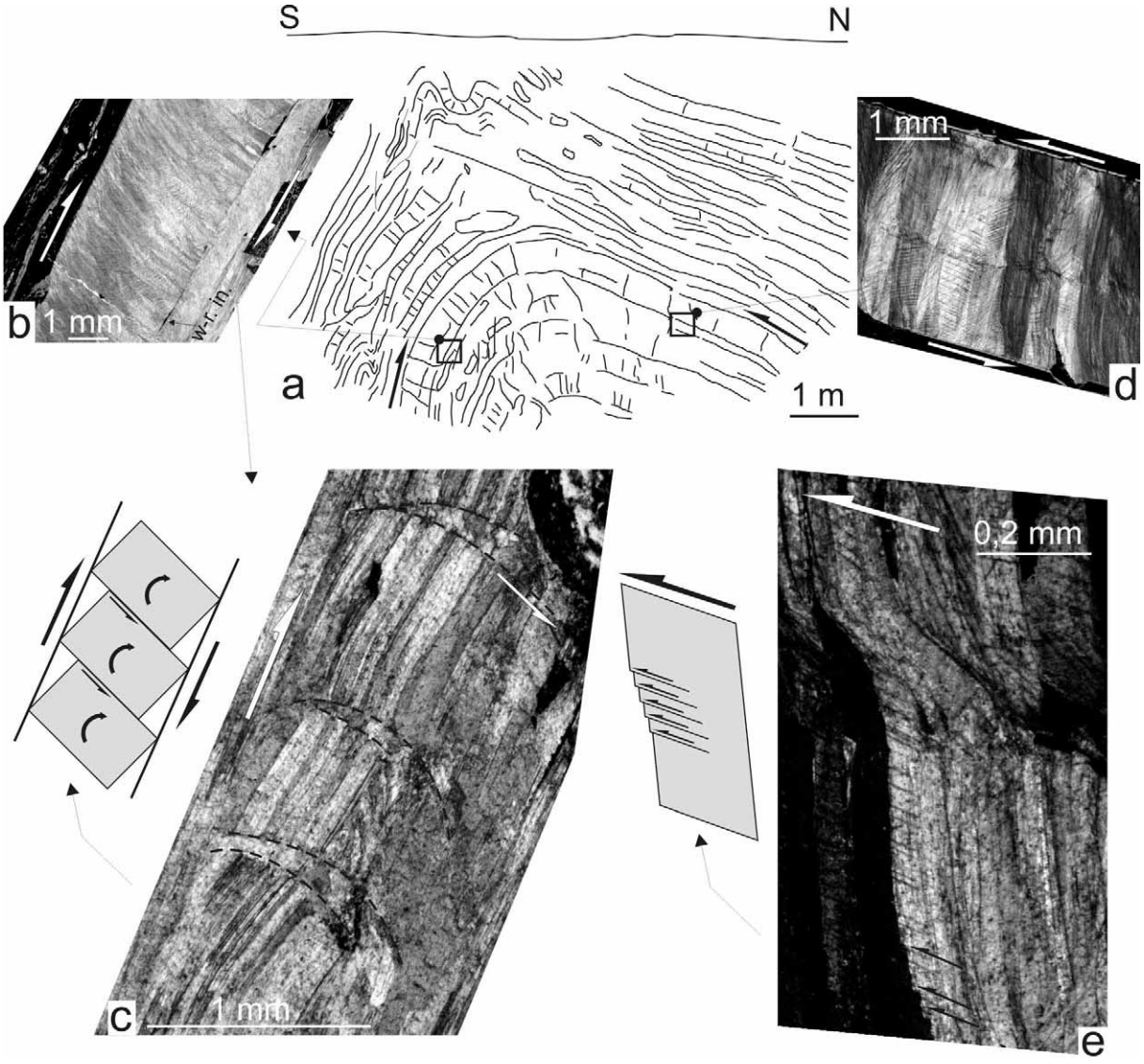

Fig. 15. Example of calcite crystal fibres on the bedding planes in the Kostomłoty Quarry. a – Sampled limbs of the anticline. b – Calcite crystal fibres from the southern limb of the anticline with wall-rock parallel inclusions (w-r. in.). c – Small blocks in the calcite vein rotated in domino style. d – Calcite crystal fibres from the northern limb of the anticline. e – fibre boundary steps. For location of quarries see Figs 2a and 4a. For other explanations see text

Compressive stress levels

For the assumed overpressures, it is possible to estimate the values of the maximum horizontal compressive stress occurring during fold growth using the equations of TWISS & MOORES (1992, their equations No 9.1.2 and 9.1.3):

$$\hat{\sigma}_1 = S + K\hat{\sigma}_3 \qquad (1)$$

where $\hat{\sigma}_1$ is the maximum compression stress, $\hat{\sigma}_3$ is the minimum principal stress, and S is the fracture strength under uniaxial compression.

$$S = \frac{2c\sin 2\Theta_f}{1+\cos 2\Theta_f} \text{ and } K = \frac{1-\cos 2\Theta_f}{1+\cos 2\Theta_f} \qquad (2)$$

where c is cohesion and Θ_f is fracture angle assumed as equal to 60°, after taking into consideration the pore fluid pressure effect.

To consider the discussed relationships, the approximate densities of rocks and their tensile strengths during folding should be known (TWISS & MOORES 1992). The current densities of carbonate and clastic rocks (ρ) from the Cambrian to the

Neogene do not change significantly and average 2.7 g cm^{-3} (PINIŃSKA 1994, 1995). Therefore, this value has been accepted for further calculations.

To estimate the values of cohesion of the Palaeozoic rocks from the initial phase of folding, laboratory-obtained tensile strengths of the rocks of different age have been compared (Text-fig. 18a).

Clastic rocks, mainly sandstones of different age from the Cambrian to the Neogene, were sampled from the Palaeozoic core and Permo-Mesozoic margin of the HCM. Comparison of the current parameters of the samples points to significant changes of values of their tensile strengths (PINIŃSKA 1994, 1995) (Text-fig. 18a). The tensile

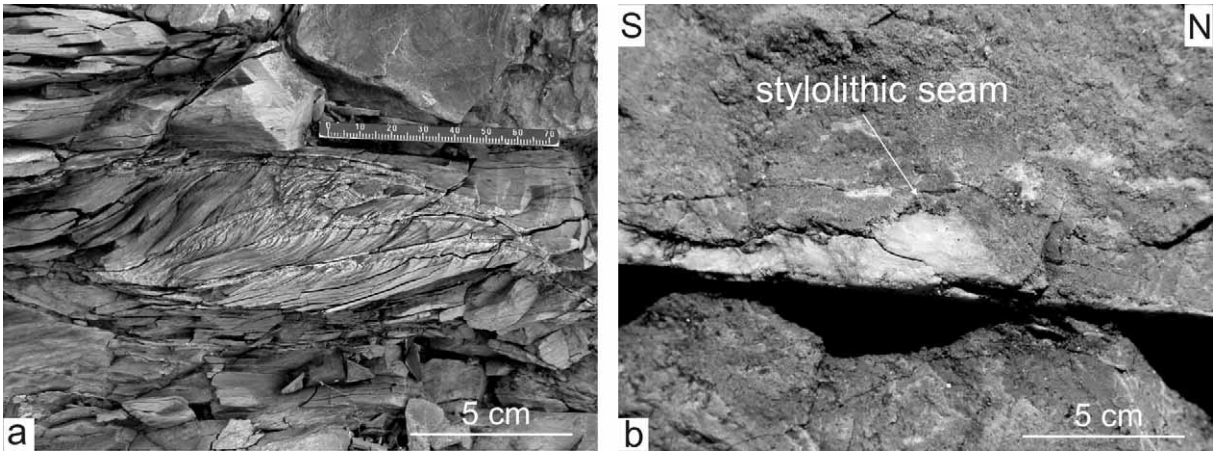

Fig. 16. Example of mesoscopic structures. a – Small scale thrust duplex from the Mogiłki Quarry. b – Stylolites from the Jaworznia Quarry. For location of quarries see Figs 2a and 4a. For other explanations see text

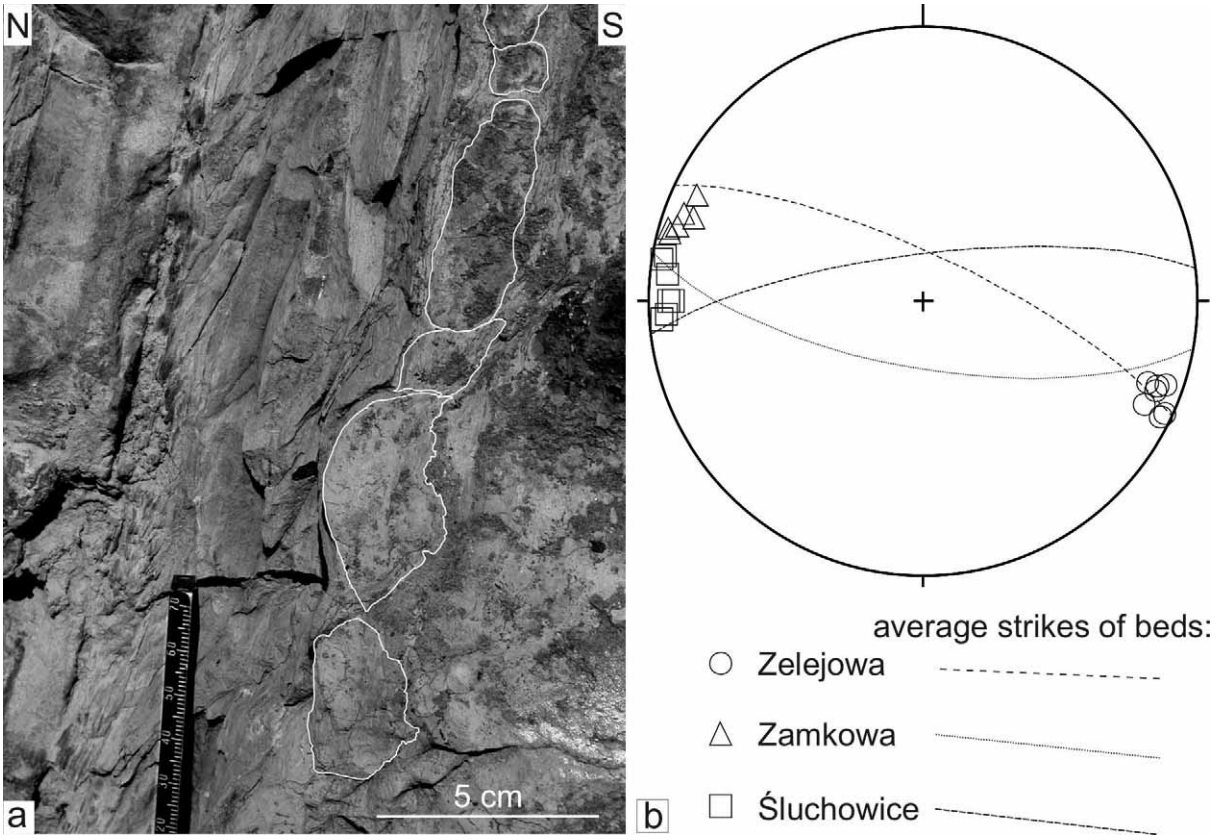

Fig. 17. Examples of boudinage. a – Single-layer boudinage from the Śluchowice Quarry. b – Diagram of axes of boudins. The average attitudes of the bedding planes marked by dashed lines. For location of quarries see Figs 2a and 4a

strengths change from 2.5 MPa, for weakly tectonically deformed Neogene rocks from the HCM area, to 15 and 20 MPa for strongly deformed Emsian and Cambrian quartzitic sandstones, respectively (PINIŃSKA 1994, 1995). This change of T is associated with the increase of the confining pressure along with depth, and the resulting change of degree of diagenesis of these rocks. Similar to the clastic rocks, the Neogene carbonate rocks from the neighbourhood of the HCM are weakly tectonically deformed and not affected by significant confining pressure, and thus are weak. Their tensile strength is close to 2 MPa. Current T does not change significantly in older Devonian carbonates from the HCM with the average equalling about 6 MPa (PINIŃSKA 1994, 1995) (Text-fig. 18a).

Comparison of the compressive strengths is needed to make further estimations of the maximum compression stress during folding. The laboratory-measured compressive strengths of the clastic rocks range from 14 to 230 MPa (Text-fig. 18b). Extremely high values of compressive strengths come only from Cambrian quartzites. The compressive strengths of the carbonate rocks do not exceed the value of 150 MPa (Text-fig. 18b).

Based on the observed changes of the strength values, it can be assumed that during the first phase of fold development, the yet undeformed Devonian carbonate and clastic rocks had rather low strength

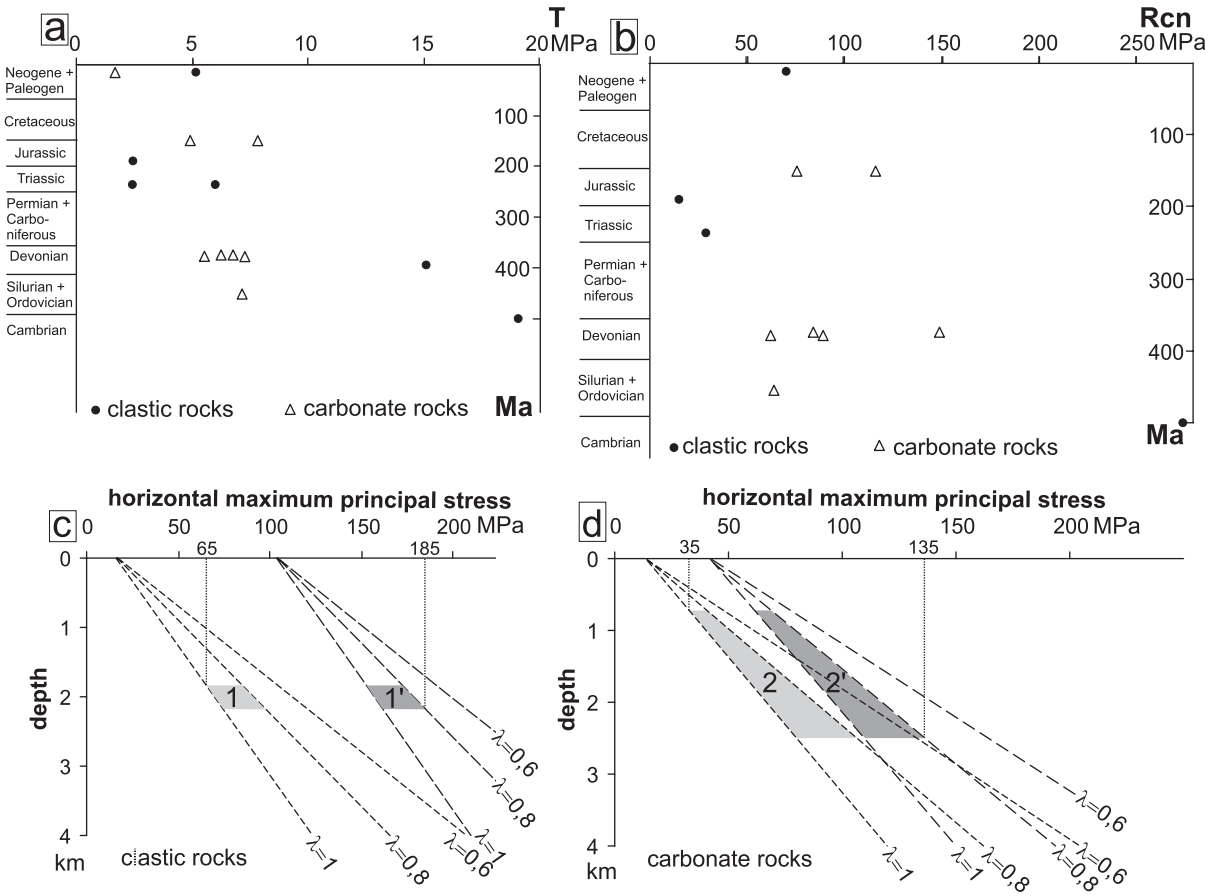

Fig. 18. a–d. Graphs showing laboratory-measured mechanical properties of rocks of different age from the HCM, based on data of PINIŃSKA (1994, 1995). Each dot and triangle displays average data calculated for each quarry, based on a dozen to a few dozen samples. a – Tensile strengths (T) of clastic and carbonate rocks. b – Compression strengths (Rcn) of clastic and carbonate rocks. c-d. Predicted variations with depth of the horizontal maximum principal stress during tectonic compression shown by lines for different values of λ for assumed high fluid pressures, based on the formulas of TWISS & MOORES (1992). c – Horizontal maximum principal stress calculated for clastic rocks. 1, 1'– intervals of approximated depth of the Devonian clastic rocks during the Early Carboniferous for different T values (light grey – 1 for T=2.5 MPa, dark grey – 1' for T=15 MPa). d – Horizontal maximum principal stress calculated for carbonate rocks. 2, 2'– intervals of approximated depth of the Devonian carbonate rocks during the Early Carboniferous for different T values (light grey – 2 for T=2 MPa, dark grey 2' for T=6 MPa). For other explanations see text

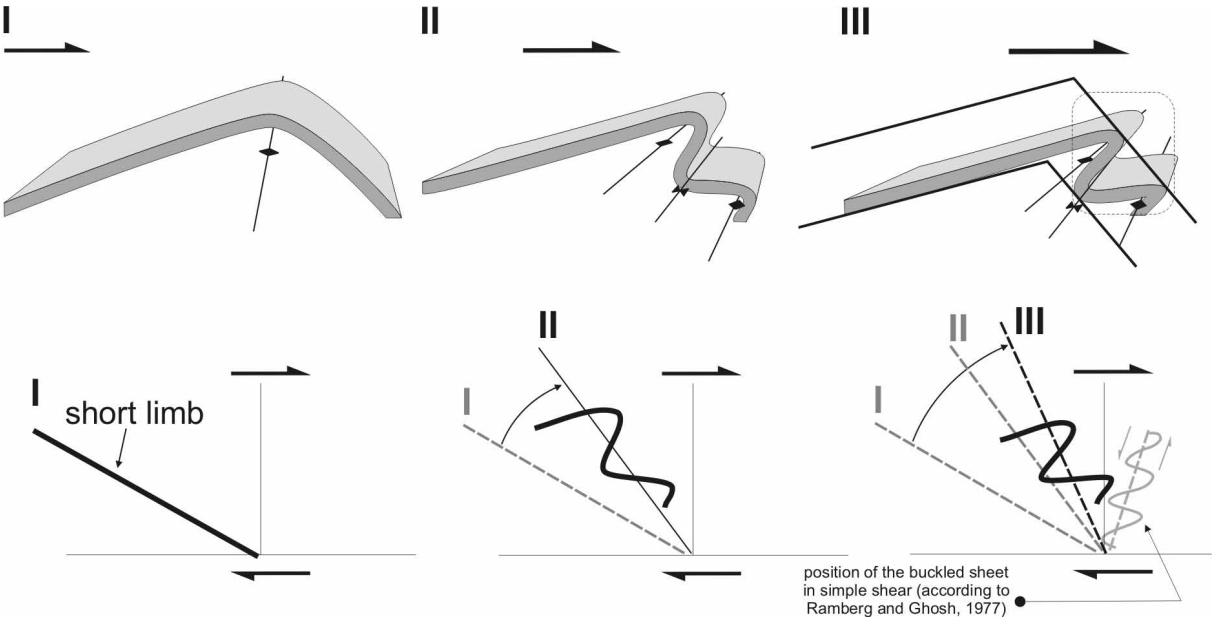

Fig. 19. Development of mesoscopic folds formed due to shortening of the short limb of a map-scale asymmetric fold. Stages of shortening of the short limb compared with the modified model of RAMBERG & GHOSH (1977) analyzing positions of the buckled sheet in simple shear

values under up to 1 km of overburden and also probably due to high fluid pressure. To make further estimate, approximate lower and upper limits of the T values were chosen for the carbonate and clastic rocks. For the clastic rocks, the lower limit was 2.5 MPa (Text-fig. 18c – 1) and upper limit was 15 MPa (Text-fig. 18c – 1'), and for the carbonate rocks 2 MPa (Text-fig. 18d – 2) and 6 MPa (Text-fig. 18d – 2'), respectively.

For these wide ranges of T, based on the formulas of TWISS & MOORES (1992), the values of the horizontal maximum compressive stress for high fluid pressures, where λ is from 0.8 to 1, were calculated (Text-figs. 18c-d). To obtain realistic values, the approximate depth range of the Devonian carbonate and clastic rocks during the Early Carboniferous are shown on the graphs (Text-figs. 4 and 18c-d).

The graphs show that for clastic rocks the range of compressive stress is from 65 to 185 MPa and for carbonate rocks – from 35 to 135 MPa (Text-figs 18c-d).

Comparison of these ranges where the ratio λ exceeded 0.8 with the laboratory-measured (PINIŃSKA 1994) current values of the compressive strengths of carbonate and clastic rocks (Text-figs 18b-d) suggests that during fold growth the maximum horizontal compressive stress was below 150 MPa. This is consistent with the upper limit of buckling stress for the majority of competent rocks, estimated to average 100 MPa (PRICE & COSGROVE 1990).

Folds

In the southern part of the HCM, map-scale thrust faults on the short limbs of the asymmetric folds, as well as on both limbs of the symmetric faulted folds suggests, that these folds could develop as thrust-related folds (see review of models in THORBJORNSEN & DUNNE 1997). These folds could precede fault propagation (e.g. break-thrust folds) or form during fault propagation. According to the criteria of MITRA (2002b), such as the occurrence of footwall synclines (e.g. Rzepka Syncline – Text-fig. 1b), common folds with a more open and rounded geometry, commonly faulted and with the geometry similar to pop-up structures (e.g. Text-figs. 4a and d) (e.g. CZARNOCKI 1956, his figs pl. 12, 21; FILONOWICZ 1967, 1970, 1973a, 1976a; HAKENBERG 1973; KOWALSKI 1975, his fig. 3a; ORŁOWSKI & MIZERSKI, 1995, their fig. 4), the folds in the Kielce Unit have a geometry similar to detachment folds (e.g. JAMISON 1987; EPARD & GROSHONG 1995; HOMZA & WALLACE 1995; MITRA 2002b; 2003).

Field and deep boreholes observations, and

refraction seismic studies (POŻARYSKI & TOMCZYK 1993) point to the occurrence of numerous faults at the transitions of strongly contrasting rock complexes, e.g. between the Silurian and Devonian strata, Silurian and Cambrian strata (e.g. CZARNOCKI 1956, his figs. 14, 15) and in the Lower Cambrian incompetent rock complex (LENDZION & *al.* 1982). This suggests that in the HCM not one distinct detachment surface was present but many second-order detachment surfaces could occur at the contacts between the competent/incompetent rocks, which are favourable horizons of detachments in many fold belts (DE SITTER 1964), a fact that has been widely documented (see broad review in MITRA 2002b, 2003).

In the Kielce-Łagów Synclinorium, south-vergent asymmetric folds prevail (e.g. FILONOWICZ 1970, 1973a, 1976 – geological cross-sections; KOWALCZEWSKI & RUBINOWSKI 1962, fig. 4; LAMARCHE & *al.* 2003), although symmetric folds also occur (e.g. CZARNOCKI 1956, pl. 12; KOWALCZEWSKI 1971, fig. 2). Asymmetric, as well as symmetric folds, are present in the Chęciny-Klimontów Anticlinorium (e.g. CZARNOCKI 1919, 1956, 1957; KOWALCZEWSKI & RUBINOWSKI 1962, fig. 4; KUTEK & GŁAZEK 1972, fig. 14; TOMCZYK 1974, fig. 39; KOWALSKI 1975, fig. 3a; LAMARCHE & *al*. 2000, fig. 1; LAMARCHE & *al*. 2003, fig. 3).

Variations in the geometry of fold profiles changing along axes in some of the folds, such as the Chęciny and Niewachlów anticlines, indicates, according to criteria of MITRA (2003), that the folds underwent shortenning of significantly different amounts.

Generally, the geometry of the folds profiles in the Kielce Unit, controlled by mechanical rock properties, display the geometry of buckle folds. Some of the mesostructures mentioned above, as e.g. F_1-F_2, F_1'-F_2', F_3-F_4, F_3'-F_4' faults and boudinage formed on the steeply-dipping limbs suggest, that during folding prevailed horizontal compression stresses parallel to the layers. The sense of movement during the development of the calcite crystal fibres also point to that the layers buckling formed by flexural-slip.

Apart from the prevailing layer-parallel shortening, layer-parallel simple shear, particularly in the late stages of development, could also occur during the development of the asymmetric folds, similar to folds in the Franciscan Complex in the San Francisco area (RAMBERG & JOHNSON 1976) that have similar lithology to the HCM. This is suggested by experimental tests of layered models by RAMBERG (1959) and GHOSH (1966) applied in investigations of the development of asymmetric folds. These tests support the view that both the component of compression parallel to the layers and the component of the layer-parallel shearing are necessary. Such a trend in the development of asymmetric folds has been observed in test models compressed at a low angle to the layering of the multilayers in the investigations of GHOSH (1968, fig. 8). However, simulations of the formation of overturned folds using finite-element analysis indicate, that these folds could form first as symmetric folds and then became asymmetrical due to shear parallel to the original horizontal (LAN & WANG 1987).

This suggests that the asymmetric folds with a distinct south-vergence, particularly close to the Holy Cross Fault, could form because of combination of layer-parallel shortening and layer-parallel shearing. The layers were probably initially shortened to form symmetric folds and in the next stages of deformation sheared because of simple shearing when the multilayers were deformed by compression at a low angle to the layering. Occurrence of layer-parallel shortening and shearing caused the development, apart from mesoscopic folds, of different mesostructures, such as flexural-slip structures and mesofaults.

In the HCM, symmetric and asymmetric mesofolds similar to the map-scale folds commonly form on the map-scale fold limbs. Change of the geometry of some of the folds was partly because of somewhat later deformation resulting from the activity of cross-fold faults. Strike separations along these faults and asymmetry of the folding in the fault blocks (e.g. Text-figs 6, 7b-c) suggest that these NW-SE striking faults are dextral strike-slip faults. The mesoscopic folds observed in the Kostomłoty and Jaźwica quarries, occurring on the limbs of the map-scale folds, developed as a result of differences in accommodation of shortening across these cross-fold faults (e.g. Text-figs 6, 7). The movement related with strike-slip faulting may result in rotation around the vertical axis, which is also confirmed in the Kostomłoty Quarry by palaeomagnetic investigations (GRABOWSKI & NAWROCKI 1996). Analysis of the radar image from the Łgawa Mt. region suggests that the fault which dissects the southern limb of the Gałęzice-Bolechowice

Syncline does not cut Upper Permian rocks on the Czerwona Góra Mt. (Text-fig. 6c). The folds and generally NW-SE striking strike-slip faults developed, as probably did other similar structures, during the late phases of the Variscan deformation. Occurrence in the Jaźwica Quarry of the second group of folds (Text-fig. 8, II group of the fold axes) is probably a result of subsequent deformation related to a younger strike-slip faulting stage.

Some of the south-verging mesoscopic folds (Text-figs 4b, 9c) formed as a result of gradual shortening of the short limbs of the asymmetric map-scale folds (Text-fig. 19, stages I→II→III) when the maximum compression axis was inclined to horizontal, similarly to the buckled sheet during simple shearing GHOSH 1966, (Figs. 10 and 11; RAMBERG & GHOSH, 1977, fig. 6).

At the end of folding or in later post-folding stage of Variscan deformation the initiated separation of the Kielce Unit along longitudinal and transverse faults resulted in changes in the trend of some of the folds. The changes being the effects of movements along these faults are suggested e.g. by palaeomagnetic investigations in some outcrops (GRABOWSKI & NAWROCKI 2001) where local tectonic rotations around the vertical axis in the Early Permian (or later) were recognized.

Mesostructures

The evolution of accommodation structures was the focus of analysis of the structures developed on the fold limbs. During the evolution of the folds in the HCM, structures developed, which according to RAMSAY (1974) and MITRA (2002a), accommodate strain variations related to changing of the structural geometry and positions of stratigraphic units during folding. Apart from typical accommodation structures such as bulbous hinge structures (RAMSAY 1974), which developed in the collapsed hinges of the folds (Text-figs 9c-d), different faults, which shortened or extended the layers, formed in the hinges as well as on the fold limbs. The proposed scheme of development of these mesofaults during the individual stages of modifications of fold shape profiles is referred here to changes of the dip angles in the limbs. In the initial phase of folding, when horizontal compression stresses probably prevailed, contraction faults developed on the fold limbs comprising conjugate symmetric F_1-F_2 sets (e.g. Text-figs 10a, 11a) preceding the development of the asymmetric F_1'-F_2' sets (e.g. Text-fig. 11b), similar to fold limbs in Lebanon (HANCOCK & ATIYA 1979).

The symmetric F_1-F_2 sets developed on shallowly dipping fold limbs, in conditions where the interlayer slip was rather small, as has been determined in laboratory tests (BEHZADI & DUBEY 1980, fig. 3). At this stage, the development of hinge wedge thrusts could also initiate in the hinge zones (Text-figs 11d-f). Further increase of the limb dips, above 30°, resulted in the increase of slip (BEHZADI & DUBEY 1980), favouring mainly the development of the F_2' fault set and a slightly weaker F_1' set. These asymmetric F_1'-F_2' faults sets developed during the increase of differential stresses associated with gradual locking of folds (HANCOCK & ATIYA 1979), resulting in higher values of the acute dihedral angles. Part of the contraction fault sets developed as limb wedge thrusts corresponding to conjugate F_1-F_2 sets on the gradually shortened short limbs of the asymmetric folds (e.g. Text-figs 11c). When the dips of these limbs increased to close to 90° (Text-fig. 12b, 1→2), single contraction fault sets developed, corresponding to the F_2 set (e.g. Text-figs 10e, j and 12), as also observed by MASTELLA (1988, fig. 24). Their formation was facilitated by a layer-parallel simple shear consisting of a flexural-slip movement (e.g. Text-fig. 12b) as observed in laboratory tests (GHOSH 1966, fig. 11). Out-of-syncline and into-anticline thrusts developed at the hinges (e.g. Text-figs 9a, b, d).

Steepening of the generally short limbs of asymmetric folds and limbs of the symmetric faulted folds caused shear away from anticline hinges on these limbs resulting in the development of forelimb shear thrusts (MITRA 2002a), the F_3-F_4 and F_3'-F_4' fault sets (e.g. Text-figs 10b, f, g, h, 12a, 13a-b). The faults of the F_3-F_4 sets developed earlier on the moderately dipping limbs, in contrast to the F_3'-F_4' sets formed on vertically dipping fold limbs (e.g. Text-fig. 13a-b).

Next, at the late stage of the modification of the asymmetric fold shapes (Text-fig. 13d, 1→2), a single extension faults set corresponding to the F_4 set formed on the overturned short limbs (e.g. Text-fig. 13d). According to investigations of RAMBERG & GHOSH (1977, fig. 7b) the sense of movement along the bedding facilitated the development of this fault set opposite to the flexural-slip sense (Text-figs 13d, e), therefore a bookshelf mechanism (MANDL 1987) could activate on such extended limbs.

Modification of fold shapes led also to the development of a series of typical structures such as cleavage, calcite crystal fibres on the bedding planes, small-scale duplexes, stylolites and boudinage (e.g. Text-figs 14-17). During buckling, the dominant deformation mechanism of folding on gradually steepening fold limbs was a flexural-slip mechanism. It resulted in the development of structures such as thrust duplexes and calcite crystal fibres. In the initial stage of the shortening of the beds, oblique-bed tectonic stylolites developed. At the late stages of fold growth, boudinage and conjugate sets of cleavage formed on the steeply-dipping limbs.

CONCLUSIONS

The study was based on structural analysis and geological maps, DEMs, radar, air-photo and satellite images. The application of these methods allowed displaying the as yet undescribed style and mechanisms of folding in the Kielce Unit, in the southern part of the Holy Cross Mountains fold belt.

The analysis has shown that the fold belt was formed by buckle folding of the sedimentary rocks complex during Variscan deformation.

The methods applied enabled determining that layer-parallel shortening initially prevailed, although layer-parallel shearing also occurred, particularly close to some of the strike-slip faults. The high pore fluid pressures ($\lambda \geq 0{,}8$), low temperatures (<150° C) and a value of horizontal compressive stress probably below 150 MPa during fold growth in the HCM favoured buckle folding. This resulted in the development of typical flexural-slip mesostructures on the limbs of the folds. Apart from these structures, different sets of contraction and extension faults, stylolites, boudinage and some cleavage sets formed as a consequence of changes of dip angles of the limbs during gradual modifications of the fold shape profiles.

In this study, the Kielce Unit was divided into smaller fault-bounded block domains, which developed at the late phase of the folding or in the post-folding stage of the Variscan deformation. This process of the offset of the Kielce Unit along transverse faults resulted in the development of sigmoidal trends of some map-scale folds between the individual block domains.

Acknowledgements

I would like to thank Jan KUTEK (Faculty of Geology, University of Warsaw) and Wesley K. WALLACE (Tectonics and SedimentationResearch Group, University of Alaska) for very helpful comments and suggestions improving the manuscript; also Leonard MASTELLA and Stanisław SKOMPSKI for useful discussions during field work. This study was supported by the Institute of Geology, Univwersity of Warsaw.

REFERENCES

BEDNARCZYK, W., CHLEBOWSKI, R. & KOWALCZEWSKI, Z. 1970. The geological structure of the northern wing of the Dyminy Anticline in Świętokrzyskie Mountains. *Bulletin of Geology,* **12**, 197-225. [*In Polish with English summary*]

BEHZADI, H. & DUBEY, A.K. 1980. Variation of interlayer slip in space and time during flexural folding. *Journal of Structural Geology*, **2**, 453-457.

BELKA, Z. 1990. Thermal maturation and burial history from conodont colour alteration data, Holy Cross Mountains, Poland. *Courier Forschung-Institut Senckenberg,* **118**, 241-251.

BERTHELSEN, A. 1993. Where different geological philosophies meet: the Trans-European Suture Zone. *In*: GEE D. G., BECKOLMEN M. (*Eds*), EUROPROBE Symposium Jablonna 1991, *Publications of the Institute of Geophysics, Polish Academy of Sciences,* **255**, 19-31.

CHESTER, J.S. 2003. Mechanical stratigraphy and fault–fold interaction, Absaroka thrust sheet, Salt River Range, Wyoming. *Journal of Structural Geology,* **25,** 1171-1192.

CLOOS, E. 1961. Bedding slips, wedges, and folding in layered sequences. *Bulletin de la Comission Géologique de Finlande*, **33**, 105-122.

COSGROVE, J. W. 1993. The interplay between fluids, folds and thrusts during the deformation of a sedimentary succession. *Journal of Structural Geology,* **15**, 491-500.

COX, S.F. 1987. Antitaxial crack-seal vein microstructures and their relationship to displacement paths. *Journal of Structural Geolog*, **9**, 779-787.

CZARNOCKI, J. 1919. Stratigraphy and tectonics of the Święty Krzyż Mountains. *Prace Towarzystwa Naukowego Warszawskiego,* **28**, 1-172. [*In Polish*]

— 1929a. O tektonice okolic Miedzianki w związku ze

złożami miedzi tegoż obszaru. *Posiedzenia Naukowe Państwowego Instytutu Geologicznego,* **24**, 29-32.

— 1929b. O tektonice okolic Łagowa oraz kilka słów w sprawie trzeciorzędu i złóż galeny na tym obszarze. *Posiedzenia Naukowe Państwowego Instytutu Geologicznego*, **24**, 32-36.

— 1938. Carte géologique générale de la Pologne, feuille 4, Kielce, Edition du Service Géologique de Pologne, scale 1:100 000.

— 1956. Surowce mineralne w Górach Świętokrzyskich. *Prace Geologiczne Instytutu Geologicznego*, **12a**, 5-108.

— 1957. Tectonics of the Święty Krzyż Mountains. Stratigraphy and tectonics of the Świety Krzyż Mountains. *Prace Geologiczne Instytutu Geologicznego*, **18**, 11-133. [*In Polish with English abstract*]

— 1961a. Materiały do przeglądowej mapy geologicznej Polski. Region Świętokrzyski. Arkusz Kielce. Wyd. B zaktualizowane, scale 1:100 000. *Wydawnictwa Geologiczne*; Warszawa.

— 1961b. Materiały do przeglądowej mapy geologicznej Polski. Region Świętokrzyski. Arkusz Bodzentyn. Wyd. B zaktualizowane, scale 1:100 000. *Wydawnictwa Geologiczne*; Warszawa.

— 1961c. Materiały do przeglądowej mapy geologicznej Polski. Region Świętokrzyski. Arkusz Opatów. Wyd. B zaktualizowane, scale 1:100 000. *Wydawnictwa Geologiczne*; Warszawa.

— 1961d. Materiały do przeglądowej mapy geologicznej Polski. Region Świętokrzyski. Arkusz Pińczów. Wyd. B zaktualizowane, scale 1:100 000. *Wydawnictwa Geologiczne*; Warszawa.

— 1961e. Materiały do przeglądowej mapy geologicznej Polski. Region Świętokrzyski. Arkusz Staszów. Wyd. B zaktualizowane, scale 1:100 000. *Wydawnictwa Geologiczne*; Warszawa.

— 1961f. Materiały do przeglądowej mapy geologicznej Polski. Region Świętokrzyski. Arkusz Sandomierz. Wyd. B zaktualizowane, scale 1:100 000. *Wydawnictwa Geologiczne*; Warszawa.

DAHLSTROM, C.D.A. 1970. Structural geology in the eastern margin of the Canadian Rocky Mountains. *Bulletin of Canadian Petroleum Geology*, **18**, 332-406.

DE SITTER, L.U. 1964. Structural Geology. Second edition, 551 pp. *McGraw-Hill*; New York.

DĘBOWSKA, U. 2004. Some aspects of tectonics and mineralization in the Devonian rocks in the western part of the Chęciny anticline: Miedzianka Mt., NW part of the Holy Cross Mts., central Poland. *Przegląd Geologiczny*, **52**, 920-927.

DOWGIAŁŁO, W.D. 1974a. Geological map of Poland, Opatów sheet, scale 1:50 000. *Wydawnictwa Geologiczne*; Warszawa.

— 1974b. Explanations to the Geological map of Poland, Opatów sheet, scale 1:50 000. *Wydawnictwa Geologiczne*; Warszawa.

EPARD J-L. & GROSHONG JR, R.H. 1995. Kinematic model of detachment folding including limb rotation, fixed hinges and layer-parallel strain. *Tectonophysics*, **247**, 85-103.

FILONOWICZ, P. 1967. Geological Map of Poland, Morawica sheet, scale 1:50 000. *Wydawnictwa Geologiczne*; Warszawa.

— 1968. Explanations to the Geological Map of Poland, Morawica sheet, scale 1:50 000. *Wydawnictwa Geologiczne*; Warszawa.

— 1970. Geological Map of Poland, Bodzentyn sheet, scale 1:50 000. *Wydawnictwa Geologiczne*; Warszawa.

— 1973a. Geological Map of Poland, Kielce sheet, scale 1:50 000. *Wydawnictwa Geologiczne*; Warszawa.

— 1973b. Explanations to the Geological Map of Poland, Kielce sheet, scale 1:50 000. *Wydawnictwa Geologiczne*; Warszawa.

— 1976a. Geological Map of Poland, Daleszyce sheet, scale 1:50 000. *Wydawnictwa Geologiczne*; Warszawa.

— 1976b. Explanations to the Geological Map of Poland, Daleszyce sheet, scale 1:50 000. *Wydawnictwa Geologiczne*; Warszawa.

FISHER, M.P. & JACKSON, P.B. 1999. Stratigraphic controls of deformation pattern in fault-related folds: a detachment fold example from the Sierra Madre Oriental, northeast Mexico. *Journal of Structural Geology*, **21**, 613-633.

GHOSH, S.K. 1966. Experimental tests of buckling folds in relation to strain ellipsoid in simple shear deformations. *Tectonophysics*, **3**, 169-185.

— 1968. Experiments of buckling of multilayers which permit inter-layer gliding. *Tectonophysics*, **6**, 207-249.

GRABOWSKI, J. & NAWROCKI, J. 1996. Multiple remagnetizations in the Devonian carbonates in the northwestern part of the Kielce region (Holy Cross Mts., southern part). *Geological Quarterly*, **40**, 47-64.

— & — 2001. Palaeomagnetism of some Devonian carbonates from the Holy Cross Mts. (central Poland): large pre-Permian rotations or strain modified palaeomagnetic directions? *Geological Quarterly*, **45**, 165-178.

GUTERCH, A., GRAD, M., KELLER, G.R., POSGAY, K., VOZAR, J., SPIČAK, A., BRUECKL, E., HAJNAL, Z., THYBO, H. & SELVI, O. 2000. The Celebration 2000 Seismic Experiment. Joint Meeting of EURO-

PROBE (TESZ) and PACE Projects. Zakopane/Holy Cross Mountains, Poland. Abstracts volume, 29-32.

GUTIÉRREZ-ALONSO, G. & GROSS, M.R. 1999. Structures and mechanisms associated with development of a fold in the Cantabrian Zone thrust belt, NW Spain. *Journal of Structural Geology*, **21**, 653-670.

HAKENBERG, M. 1973. Geological Map of Poland, Chęciny sheet, scale 1:50 000. *Wydawnictwa Geologiczne*; Warszawa.

— 1974. Explanations to the Geological Map of Poland, Chęciny sheet, scale 1:50 000. *Wydawnictwa Geologiczne*; Warszawa.

HAKENBERG, M., KUTEK, J., MATYJA, B., MIZERSKI, W., RUTKOWSKI, J., STUPNICKA, E., ŚWIDROWSKA, J. & TRAMMER, J. 1976. Stratygrafia, wykształcenie litologiczne i tektonika mezozoiku południowo-zachodniego obrzeżenia Gór Świętokrzyskich. *In*: POŻARYSKI W. (*Ed.*), *Przewodnik 47 Zjazdu Polskiego Towarzystwa Geologicznego*, 185-202.

HANCOCK, P.L. 1985. Brittle microtectonics: principles and practise. *Journal of Structural Geology*, **7**, 437-457.

HANCOCK, P.L. & ATIYA, M.S. 1979. Tectonic significance of mesofracture systems associated with the Lebanese segment of the Dead Sea transform fault. *Journal of Structural Geology*, **1**, 143-153.

HOMZA, T.X. & WALLACE, W.K. 1995. Geometric and kinematic models of detachment folds with fixed and variable detachment depths. *Journal of Structural Geology*, **37**, 575-588.

HORNE, R. & CULSHAW, N. 2001. Flexural-slip folding in the Meguma Group, Nova Scotia, Canada. *Journal of Structural Geology*, **23**, 1631-1652.

JAMISON, W.R. 1987. Geometric analysis of fold development in overthrust terranes. *Journal of Structural Geology*, **9**, 207-219.

JAROSZEWSKI, W. 1972. Mesoscopic structural criteria of tectonics of non-orogenic areas: an example from the north-eastern Mesozoic margin of the Świętokrzyskie Mountains. *Studia Geologica Polonica*, **37**, 9-210. [*In Polish*]

JESSELL, M.W., WILLMAN, C.E. & GRAY, D.R. 1994. Bedding parallel veins and their relationship to folding. *Journal of Structural Geology*, **16**, 753-767.

KONON, A. & ŚMIGIELSKI, M. 2006. DEM-based structural mapping (examples from the Holy Cross Mountains and the Polish Outer Carpathians). *Acta Geologica Polonica*, **56** (1), 1-16.

KOWALCZEWSKI, Z. 1971. Główne rysy tektoniki Gór Świętokrzyskich. *Przewodnik 43 Zjazdu PTG*, 10-19.

KOWALCZEWSKI Z. & RUBINOWSKI Z. 1962. Główne elementy tektoniczne paleozoiku antyklinorium świętokrzyskiego. *Przegląd Geologiczny*, **9**, 451-456.

KOWALSKI, W.R. 1975. Tectonics of the western end of Chęciny anticline and surrounding structures of Mesozoic margins of the Holy Cross Mts. *Rocznik Polskiego Towarzystwa Geologicznego*, **45**, 45-61.

KUTEK, J. 2001. The Polish Permo-Mesozoic Rift Basin. *In*: ZIEGLER, P.A., CAVAZZA, W., ROBERTSON, A.H.P. & CRASQUIN-SOLEAU (*Eds*), Peri-Tethyan Rift/Wrench Basins and Passive Margins. Peri-Tethys Memoir 6, *Mémoires du Muséum National d'Histoire Naturelle*, **186**, 213-236.

KUTEK, J. & GŁAZEK, J. 1972. The Holy Cross area, Central Poland, in the Alpine cycle. *Acta Geologica Polonica*, **22**, 603-653.

LAMARCHE, J., MANSY, J. L., BERGERAT, F., AVERBUCH, O., HAKENBERG, M., LEWANDOWSKI, M., STUPNICKA, E., ŚWIDROWSKA, J., WAJSPRYCH, B. & WIECZOREK, J. 1999. Variscan tectonics in the Holy Cross Mountains (Poland) and the role of structural inheritance during Alpine tectonics. *Tectonophysics*, **313**, 171-186.

LAMARCHE, J., MANSY, J. L., SZULCZEWSKI, M. & LEWANDOWSKI, M. 2000. Pre-Variscan, Variscan and Alpine partitioning deformation in the Holy Cross Mts. (Poland). Joint Meeting of EUROPROBE (TESZ) and PACE Projects. Zakopane/Holy Cross Mountains, Poland. Abstracts volume, 56-59.

LAMARCHE, J., BERGERAT, F., LEWANDOWSKI, M., MANSY, J.L, ŚWIDROWSKA, J. & WIECZOREK, J. 2002. Variscan to Alpine heterogenous palaeo-stress field above a major Palaeozoic suture in the Carpathian foreland (southeastern Poland). *Tectonophysics*, **357**, 55-80.

LAMARCHE, J., LEWANDOWSKI M., MANSY, J.L. & SZULCZEWSKI, M. 2003. Partitioning pre-, syn- and post-Variscan deformation in the Holy Cross Mountains, eastern Variscan foreland. *In*: MCCANN, T. & SAINTOT, A. (*Eds*), Tracing tectonic deformation using the sedimentary record. *Geological Society, London, Special Publications*, **208**, 159-184.

LAN, L. & WANG, R. 1987. Finite-element analysis of an overturned fold using a viscous-fluid model. *Tectonophysics*, **139**, 309-314.

LENDZION, K., MOCZYDŁOWSKA, M. & ŻAKOWA, H. 1982. A new look at the Bazów Cambrian Sequence (southern Holy Cross Mts). *Bulletin of the Polish Academy of Sciences, Earth Sciences*, **30**, 67-75.

MALINOWSKI, M., ŻELAŹNIEWICZ, A., GRAD, M., GUTERCH, A. & JANIK, T. 2005. Seismic and geological structure of the crust in the transition from Baltica to Palaeozoic Europe in SE Poland – CELEBRA-

TION 2000 experiment, profile CEL02. *Tectonophysics*, **401**, 55-77.

MANDL, G. 1987. Tectonic deformation by rotating parallel faults: the "bookshelf" mechanism. *Tectonophysics*, **141**, 277-316.

MARYNOWSKI, L. 1997. Stopień dojrzałości materii organicznej ze skał węglanowych dewonu Gór Świętokrzyskich. *Przegląd Geologiczny*, **45**, 899-903.

MASTELLA, L. 1988. Structure and evolution of Mszana Dolna Tectonic Window, Outer Carpathians, Poland. *Annales Societatis Geologorum Poloniae*, **58**, 53-173. [*In Polish with English abstract*]

MASTELLA, L. & MIZERSKI, W. 2002. Geological setting of the Łysogóry Unit (Holy Cross Mountains, Central Poland) based on analysis of the radar images.. *Przegląd Geologiczny*, **50**, 767-772. [*In Polish with English abstract*]

MITRA, S. 2002a. Fold-accommodation faults. *American Association of Petroleum Geologists Bulletin*, **86**, 671-693.

— 2002b. Structural models of faulted detachment folds. *American Association of Petroleum Geologists Bulletin*, **86**, 1673-1694.

— 2003. A unified kinematic model for the evolution of detachment folds. *Journal of Structural Geology*, **25**, 1659-1673.

MIZERSKI, W. 1995. Geotectonic evolution of the Holy Cross Mts in Central Europe. *Biuletyn PIG* **372**, 5-47.

MIZERSKI, W. & ORŁOWSKI, S. 1993. Main transversal faults and their importance for the tectonic of the Klimontów Anticlinorium (Holy Cross Mts). *Geological Quarterly*, **37**, 19-40.

NORRIS, D.K. 1958. Structural conditions in Canadian coal mines. *Bulletin of the Geological Survey of Canada*, **44**, 1-54.

ORŁOWSKI, S. 1975. Cambrian and Upper Precambrian lithostratigraphic units in the Holy Cross Mts. *Acta Geologia Polonica*, **25**, 431-446. [*In Polish*]

ORŁOWSKI, S. & MIZERSKI, W. 1995. New data on geology of the Middle Cambrian rocks in the Klimontów Anticlinorium (Holy Cross Mts.). *Geological Quarterly*, **39**, 293-306.

— & — 1996. The Cambrian rocks and their tectonic evolution in the Dyminy Anticline of the Holy Cross Mts.. *Geological Quarterly*, **40**, 353-366.

PEACKOCK, D.C. P. & SANDERSON, D.J. 1992. Effects of layering and anisotropy on fault geometry. *Journal of the Geological Society, London*, **149**, 793-802.

PINIŃSKA, J. (*Ed*.) 1994. Właściwości wytrzymałościowe i odkształceniowe skał. Skały osadowe regionu świętokrzyskiego, 1. Zakład Geomechaniki IHiGI Wydział Geologii Uniwersytetu Warszawskiego. Warszawa

— (*Ed*.) 1995. Właściwości wytrzymałościowe i odkształceniowe skał. Skały osadowe regionu świętokrzyskiego, 2. Zakład Geomechaniki IHiGI Wydział Geologii Uniwersytetu Warszawskiego. Warszawa.

POŻARYSKI, W. 1969. Podział obszaru Polski na jednostki tektoniczne. *Przegląd Geologiczny*, **2**, 57-65.

— 1978. The Świętokrzyski Massif. *In*: Geology of Poland, 4 Tectonics, pp. 216-227. *Wydawnictwa Geologiczne*; Warszawa.

— 1990. Kaledonidy środkowej Europy – orogenem przesuwczym złożonym z terranów. *Przegląd Geologiczny,* **38**, 1-9.

— 1992. Mapa tektoniczna Polski w epoce waryscyjskiej. *Przegląd Geologiczny,* **40**, 643-651.

POŻARYSKI, W. & TOMCZYK, H. 1993. Przekrój geologiczny przez Polskę południowo-wschodnią. *Przegląd Geologiczny* **41**, 687-695.

PRICE, N.J. & COSGROVE, J.W. (*Eds*) 1990. Analysis of geological structures, pp. 1-502. *Cambridge University Press*; Cambridge.

RACKI, G. & ZAPAŚNIK, T. 1979. Uwagi o tektonice utworów dewońskich synkliny gałęzickiej. *Przegląd Geologiczny* **3**, 154-158.

RAMBERG, H. 1959. Evolution of ptygmatic folding. *Norsk Geologisk Tidsskrift*, **39**, 99-152.

RAMBERG, I.B. & JOHNSON, A.M. 1976. Asymmetric folding in interbedded chert and shale of the Franciscan Complex, San Francisco Bay Area, California. *Tectonophysics*, **32**, 295-320.

RAMBERG, H. & GHOSH, S.K. 1977. Rotation and strain of linear and planar structures in three-dimensial progressive deformation. *Tectonophysics*, **40**, 309-337.

RAMSAY, J.G. 1967. Folding and fracturing of rocks, 568 pp. *McGraw-Hill*; New York.

— 1974. Development of chevron folds. *Geological Society of America Bulletin*, **85**, 1741-1754.

RAMSAY, J.G. & HUBER, M.I. 1987. The Techniques of Modern Structural Geology. Volume 2: Folds and Fractures. *Academic Press*; London.

ROMANEK, A. 1977. Explanations to the Geological map of Poland, Klimontów sheet, scale 1:50 000. *Wydawnictwa Geologiczne*; Warszawa.

SAMSONOWICZ, J. 1926. Uwagi nad tektoniką i paleogeografią wschodniej części masywu paleozoicznego Łysogór. *Posiedzenia Państwowego Instytutu Geologicznego*, **15**, 44-46.

— 1934. Explication de la feuille Opatów. Carte

Géologique Générale de la Pologne au 100 000. Varsovie.

STUPNICKA, E. 1986. Structural characteristic of Cambrian in the western part of the Chęciny anticline (Holy Cross Mts). *Bulletin of Geology*, **30**, 61-82.

— 1992. The significance of the Variscan orogeny in the Świętokrzyskie Mountains (Mid-Polish Uplands). *Geologishe Rundschau*, **81**, 561-570.

SZULCZEWSKI, M. 1995. Depositional evolution of the Holy Cross Mts. (Poland) in the Devonian and Carboniferous – a review. *Geological Quarterly*, **39**, 471-488.

TANNER, P.W.G. 1989. The flexural-slip mechanism. *Journal of Structural Geology*, **11**, 635-665.

— 1992. Morphology and geometry of duplexes formed during flexural-slip folding. *Journal of Structural Geology*, **14**, 1173-1192.

TARNOWSKA, M. 1981. Dewon dolny w centralnej części Gór Świętokrzyskich. *Przewodnik 53 Zjazdu PTG*, 57-68.

TOMCZYK H. 1974. Góry Świętokrzyskie. *In*: POŻARYSKI W. (*Ed*.) Budowa geologiczne Polski. Tektonika, pp. 128-197. *Wydawnictwa Geologiczne*; Warszawa.

— 1988. Region łysogórski a platforma wschodnioeuropejska w cyklu kaledońsko-waryscyjskim. *Przegląd Geologiczny*, **1**, 9-17.

THORBJORNSEN, K.L. & DUNNE, W.M. 1997. Origin of a thrust-related fold: geometric vs kinematic tests. *Journal of Structural Geology*, **19**, 303-319.

TWISS, R.J. & MOORES, E.M. 1992. Structural Geology. *W. H. Freeman and Company*; New York.

UNRUG, R., HARAŃCZYK, CZ. & CHOCYK-JAMIŃSKA, M. 1999. Easternmost Avalonian and Armorican-Cadomian terranes of central Europe and Caledonian-Variscan evolution of the polydeformed Kraków mobile belt: geological constraints. *Tectonophysics*, **302**, 133-157.

WALCZOWSKI, A. 1966. Geological Map of Poland, Łagów sheet, scale 1:50 000. *Wydawnictwa Geologiczne*; Warszawa.

— 1968. Explanations to the Geological map of Poland, Łagów sheet, scale 1:50 000. *Wydawnictwa Geologiczne*; Warszawa.

ZNOSKO, J. 1962. W sprawie nowego nazewnictwa jednostek tektonicznych Gór Świętokrzyskich. *Przegląd Geologiczny*, **9**, 455-456.

Manuscript submitted: 25th February 2006
Revision version accepted: 10th September 2006